# Combined Experimental and Theoretical Determination of Effective Wake for a Marine Propeller

by

Todd Eric Taylor

A.B., Bowdoin College (1990)

Submitted to the Department of Ocean Engineering
in partial fulfillment of the requirements for the degree of

Master of Science in Ocean Engineering

at the

MASSACHUSETTS INSTITUTE OF TECHNOLOGY

February 1994



Author .....
Department of Ocean Engineering
October 18, 1993

Certified by .....
Justin E. Kerwin
Professor of Naval Architecture
Thesis Supervisor

Accepted by .....
Professor A. Douglas Carmichael
Chairman, Departmental Committee on Graduate Students

# Combined Experimental and Theoretical Determination of Effective Wake for a Marine Propeller

by

Todd Eric Taylor

Submitted to the Department of Ocean Engineering
on October 18, 1993, in partial fulfillment of the
requirements for the degree of
Master of Science in Ocean Engineering

## Abstract

Marine propellers operate behind a ship in a spatially varying flow field which deviates from free stream largely due to the viscous and form drag of the hull underbody. While current theoretical design and analysis methods can work well for propellers which will operate in relatively uniform flow, this is often not the case for propellers designed to operate in a highly non-uniform wake.

Experiments were carried out at the MIT Marine Hydrodynamics Water Tunnel to determine the nominal and total wake behind a scale model ship. The model, along with a wake screen, served as a wake generator to provide velocity profiles representative of modern, high powered, single-screw containerships. The effective wake was determined by subtracting theoretically calculated propeller-induced velocities from the experimentally determined total wake. While previous investigations in this area of marine propeller design have concentrated on representation of the effective wake as a function of radius alone, this research represents the model scale three-dimensional nominal, effective, and total wake velocities as functions of both radial and circumferential location.

Thesis Supervisor: Justin E. Kerwin
Title: Professor of Naval Architecture

# Acknowledgments

Many thanks go to Professor Justin Kerwin for his guidance and encouragement throughout this project. Dr. Charles Mazel was instrumental in the experimental set-up and data acquisition procedures and the solution of all types of associated difficulties. Mr. B. Matthew Knapp deserves special recognition for his endless hours and boundless sense of humor.

Thanks go to the Hyundai Maritime Research Institute, especially Dr. Keh-Sik Min and Dr. Hong-Gi Lee, for project support and guidance. My studies at MIT have been funded by the Office of Naval Research Graduate Fellowship Program, administered by the American Society for Engineering Education.

# Contents

# List of Figures

# List of Tables

# Chapter 1

# Introduction

## 1.1 Background

It is our understanding that major shipbuilders have experienced difficulty in predicting the performance of propellers for modern high powered single screw ships. While current theoretical design and analysis methods appear to work well for propellers which operate in relatively uniform inflow, this is not often the case for propellers designed to operate in a highly non-uniform wake.

## 1.2 Purpose

The purpose of this project is to develop improved technology for designing more efficient propulsors for these vessels. The approach has been an in-depth experimental and theoretical study of a typical high powered containership, carried out jointly by Hyundai Maritime Research Institute(HMRI) and MIT. The research concentrates on representation and comparison of the model scale nominal, effective, and total wakes.

# Chapter 2

# Experimental Procedure

## 2.1 The Water Tunnel

The MIT Marine Hydrodynamics Water Tunnel is a closed-loop tunnel driven by a single impeller connected to a 75 horsepower electric motor. The pressure in the tunnel can be lowered with a vacuum pump to aid in applications such as cavitiation studies. The entire water tunnel has a square profile two stories high. The test section, which is at the top of the loop, is four feet long and has a cross-section twenty inches(508 mm) square. Maximum velocity of the water is about 30 feet/second in the forward direction and near 15 feet/second in reverse. Upstream of the test section is a 5:1 contraction section fitted with a honeycomb mesh with circular cells of 0.71 inch diameter, and a wake screen(0.035 inch wire, 6 wires per inch) to promote flow uniformity. The test section has removable Plexiglass windows on all four sides for ease of assembling and viewing experiments.

A propeller shaft can be extended from upstream, through the honeycomb, into the test section. The propeller shaft consists of a stationary outer fairing housing an inner rotating drive shaft. Propellers are mounted on the downstream end of the drive shaft. Propeller thrust and torque can be measured from load cells mounted on the upstream end of the shaft. Performance of a propeller at various operating conditions can be simulated in the water tunnel by varying the impeller (water speed) and propeller (propeller RPM) settings. The nominal water speed in the tunnel test

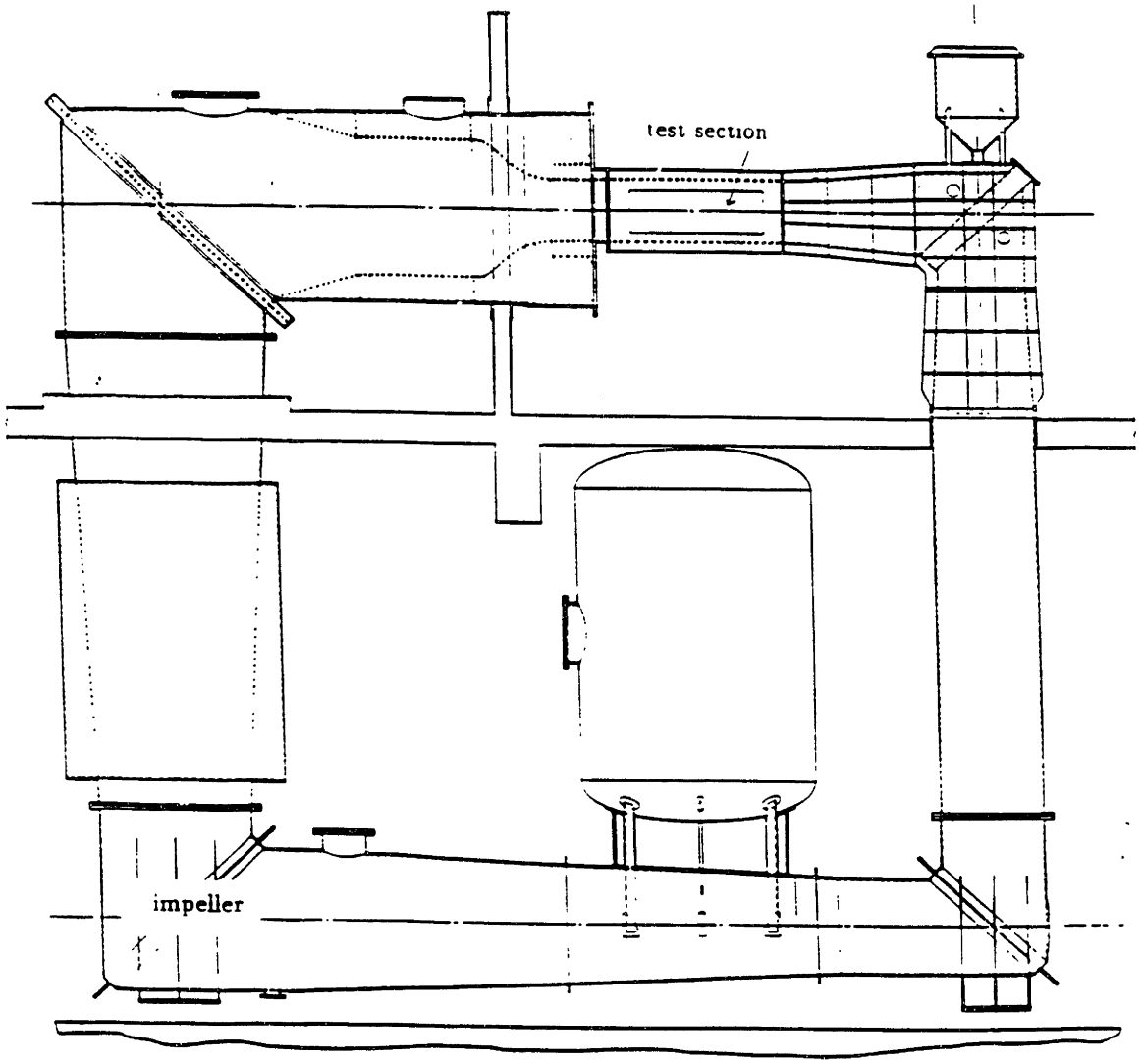


Figure 2-1: MIT Water Tunnel

section is measured by a pair of differential pressure cells in the contraction section. Software available in the facility can provide information on propeller performance in terms of advance coefficient, thrust coefficient, torque coefficient, and efficiency. The propeller drive shaft is driven by a 40 horsepower electric motor.

Water velocities in the test section are measured using laser Doppler velocimetry(LDV) through a laser quality plexiglass test section window. LDV is a non-intrusive technique using the analysis of laser light scattered by particles in a flow to measure the fluid velocity. The MIT Water Tunnel uses a three watt argon-ion Lexel Model 95 laser. See [3] for a description of LDV in general or [2] for the specifics of the MIT Water Tunnel system.

## 2.2 Wake Generator

The conceptual design of the model/wake generator was developed by correspondence between HMRI and MIT. Detailed design and construction were carried out by HMRI. Considerations in the design were:

1. It should represent the key features of a modern containership wake field.
2. It should be easily rotated without disassembly while in the test section.
3. The upper portion of the hull should not block the laser beams.
4. The design should fit in both the HMRI and MIT tunnels to allow similar (comparative) studies at the two facilities.

The wake generator consisted of a model containership underbody and a wake screen.

### 2.2.1 Containership Underbody Model

A scale model, representative of a modern containership underbody, was constructed from closed cell polyurethane foam and resin over six wooden frames. The outer surface of the model was coated with paint which provided a very smooth finish

to the foam/resin surface. The model was constructed with a large hole through each of the wooden frames, as well as holes in the bow and stern, which allowed the model to be slid over the non-rotating outer fairing surrounding the propeller shaft. With this configuration, the bow of the model pointed upstream into the flow and the stern of the model ended at the downstream end of the propeller drive shaft. When mounted on the drive shaft, the model propeller was thus located in a position representative of a properly configured full scale hull/propeller(See Figure 2-3). The model was prevented from moving fore and aft and/or rotating about the propeller shaft during the experiment by six set screws through the model, just forward of the model propeller, into the fairing.

### 2.2.2 Wake Screen

In most situations, a propeller operates behind a ship in a flow field which deviates from free stream largely due to the viscous and form drag of the hull underbody. In general, this influence of the hull on the flow field is due primarily to viscous effects. The wake screen was included as part of the wake generator because it is often not possible to generate a large enough wake defect by means of the viscous and form drag of a model hull alone.

The wake screen was made from screen of varying mesh sizes. The entire screen was mounted on a brass ring with a diameter of 480mm. The ring was streamlined(foil shaped) in cross-section with a chord of 50mm and a thickness of 5mm.

### 2.2.3 Model Propeller

A model propeller was constructed of #2024-T4 aluminum to the same scale as the underbody model. The propeller was anodized with black "hard-coat" to fight corrosion. The propeller dimensions are given in Appendix C, and a computer depiction of the full scale propeller geometry is shown in Figure 2-4. Depending on the particular experimental measurements taking place, the model propeller can be run in place behind the underbody model or the propeller can be replaced by a dummy hub.

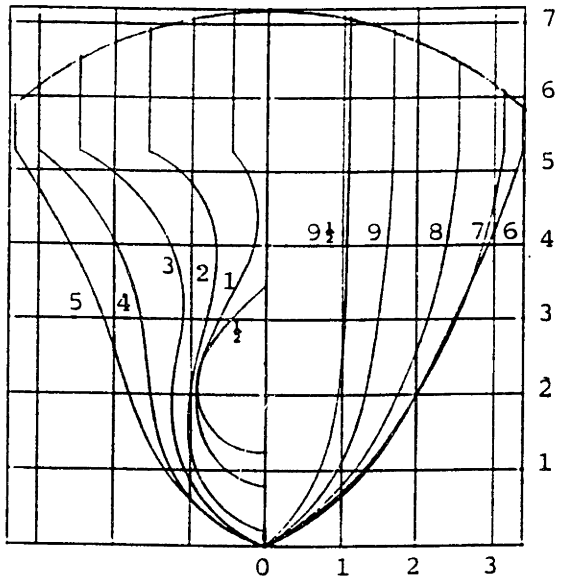


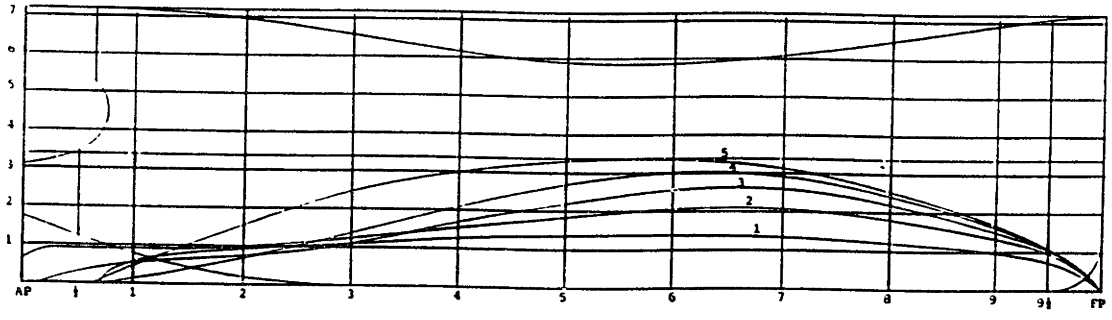


Figure 2-2: Line Drawings of Containership Underbody Model

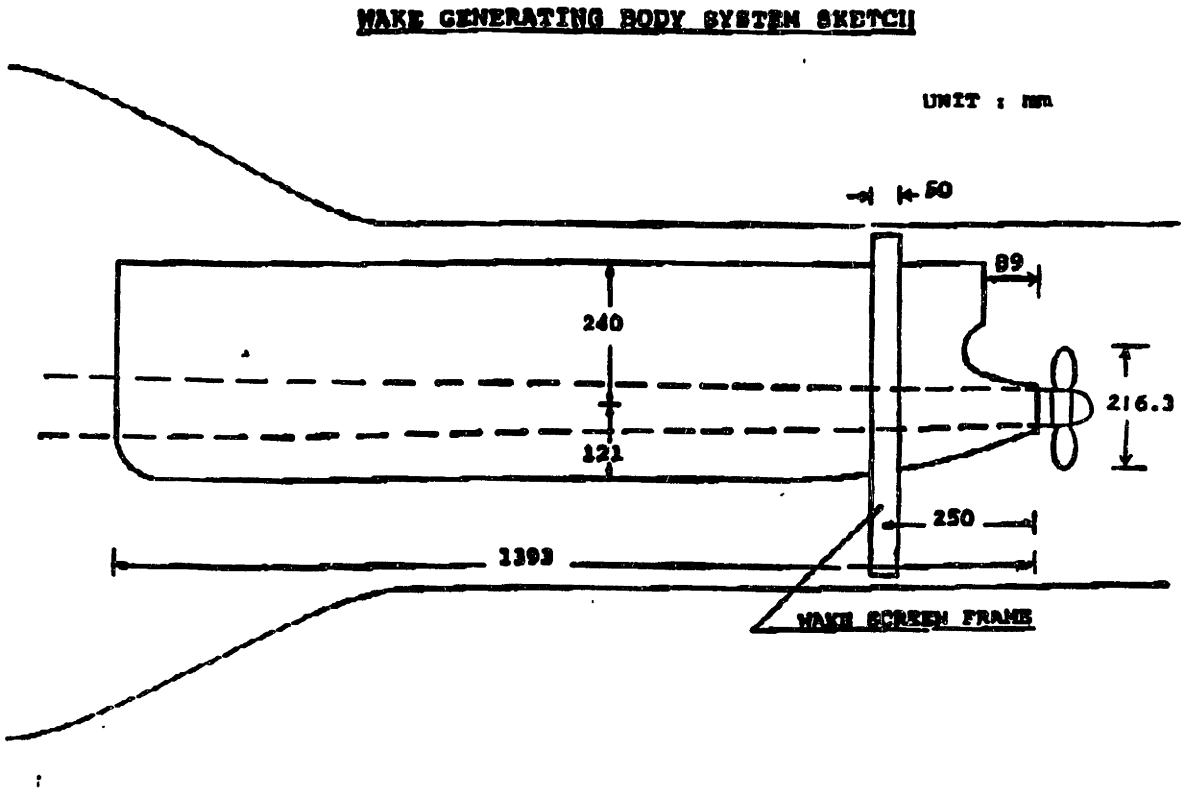


Figure 2-3: Wake Generator and Model Propeller Mounted on Propeller Shaft

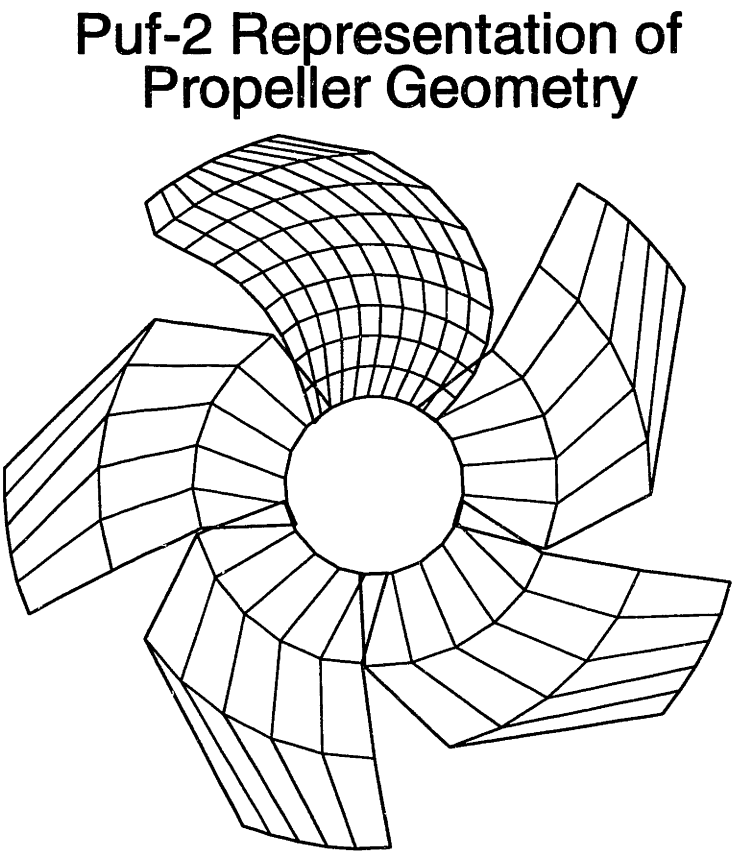


Figure 2-4: Puf-2 Representation of Propeller Geometry

## 2.3 Determination of Nominal Wake

### 2.3.1 Initial Tests

With the dummy hub used in place of the propeller, an initial LDV wake survey was carried out in the plane of the propeller. The results were disappointing when compared with the target wake distribution provided by an HMRI towing tank/5-hole pitot measurement. The target wake distribution is a map of axial velocities(downstream velocities, parallel to the centerline of the model) provided by HMRI as representative of the distribution of axial velocities in the wake of a typical single-screw containership(See Figure 2-5). In this initial survey, a substantial wake deficit existed at the bottom of the propeller disk. Detailed LDV traverses were carrried out upstream of the propeller plane, and also the flow in this region was visualized by lowering the tunnel pressure to create bubbles. Both techniques indicated that flow separation was taking place at the bottom of the model just forward of the plane of the propeller(See Figure 2-6).

Upon consultation with HMRI, portions of the wake screen were removed, and the wake survey was repeated at the propeller plane. This process was repeated several times until the flow separation problem was cured and a satisfactory wake pattern was achieved(See Figures 2-7 and 2-8).

### 2.3.2 LDV Measurements

After additional initial testing it was found that measurements taken on the side of the model farthest from the laser were occasionally difficult due to laser power losses to the water. Also, in substantial areas on the far side of the test section, the laser beams were blocked by portions of the hull, propeller hub, and fairwater. Thus, it was only practical to take LDV measurements in the half-plane of the test section closest to the laser.

Easy rotation of the model around the propeller shaft allowed LDV measurements from any angle relative to the model. As it was not practical or necessary to study the

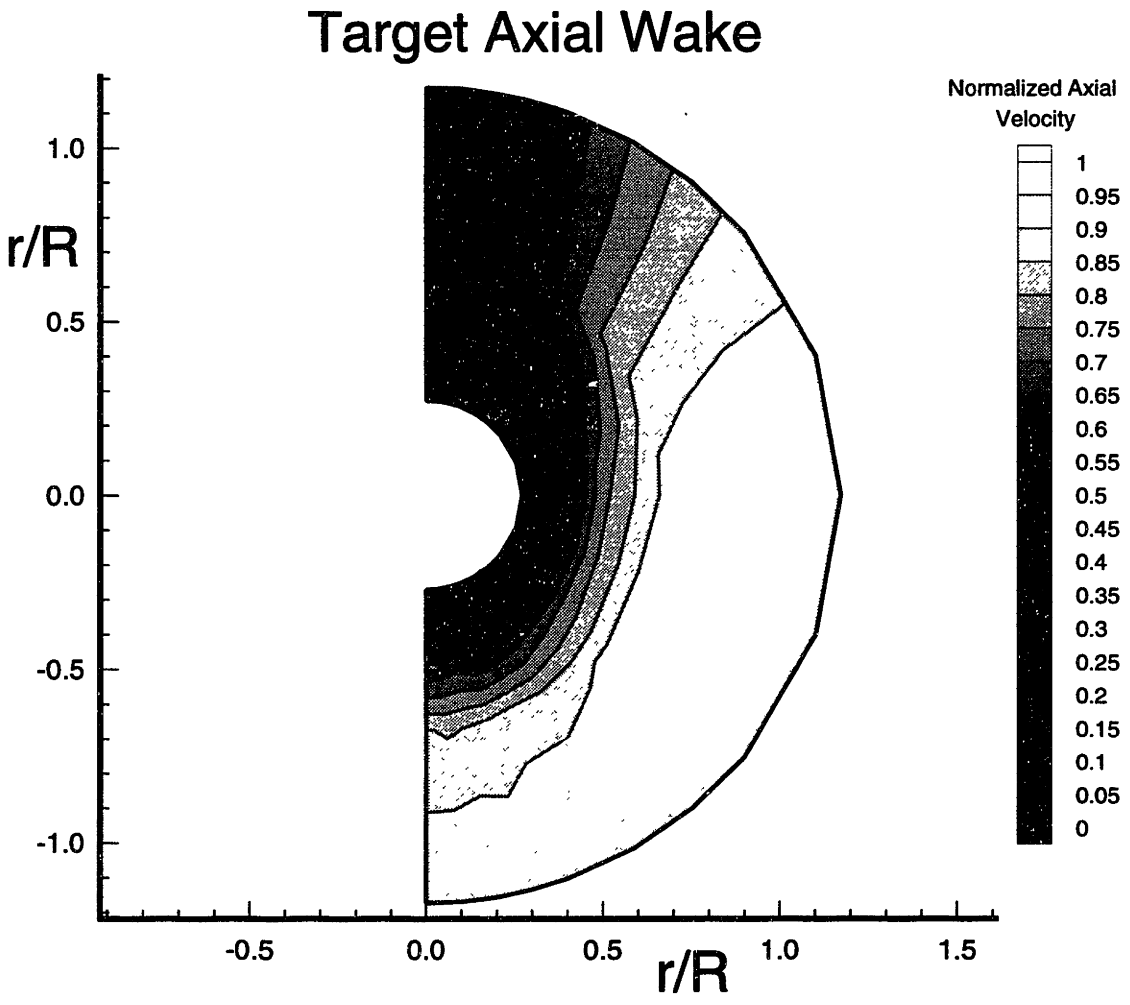


Figure 2-5: HMRI Target Axial Wake Distribution

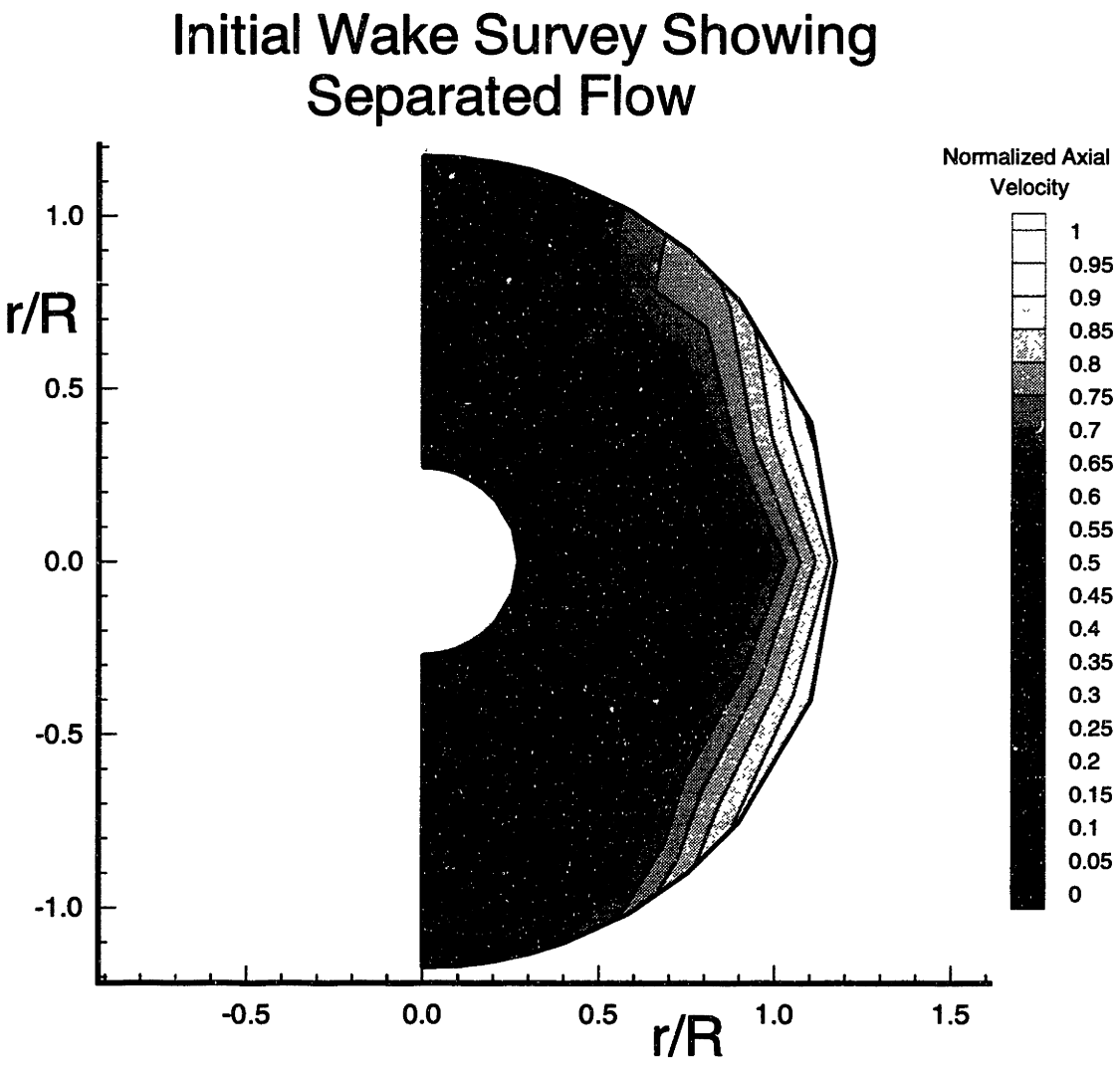


Figure 2-6: Initial LDV Wake Survey

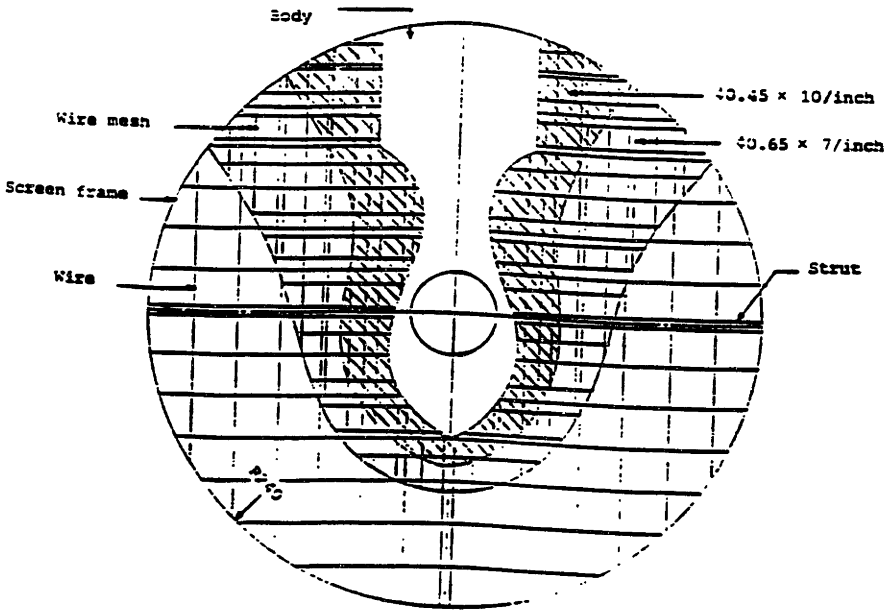


**Figure 2-8: Original Wake Screen**

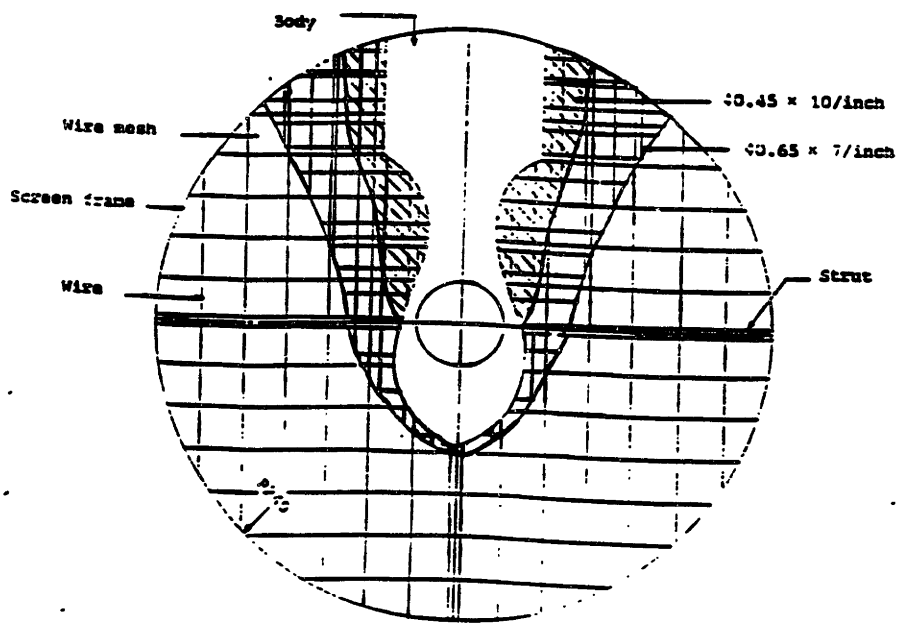


**Figure 2-9: Final Wake Screen Configuration**

model flow from every angle, screws through the wake screen ring into small mounts, attached to three of the four windows of the test section, facilitated mounting of the wake screen(and thus the entire model) in each of only four angular positions. These positions were: upright(0 degree rotation,port side towards laser), deck towards laser(90 degree rotation), inverted(180 degree rotation,starboard side towards laser), and keel to laser(270 degree rotation). Obviously, these positions differ by multiples of 90 degrees. Due to the square cross-section of the test section of the water tunnel, the 90 degree increments of model roation, and the fact that the propeller shaft was braced so that its logitudinal axis was held in the center of the test section at each location, the location of the tunnel walls(symmetric in each of the four directions) relative to the model was expected to be identical for each 90 degree increment of model rotation. Thus the flow relative to the model for each rotation of the model was expected to be the same.

The laser system used by the MIT Water Tunnel allowed water velocity measurements to be taken only in the axial(downstream) and vertical directions, relative to the laser and tunnel. With this arrangement, axial and vertical velocities(relative to the tunnel) were taken in the near side half-plane of the test section for each of the four rotation positions of the model/wake generator. In order to fully describe the flows, though, three-dimensional velocity components at each given point are necessary.

For a given point, relative to the model, axial velocity measurements taken during two different rotations are redundant. Vertical velocities, relative to the tunnel, may be resolved to either vertical or horizontal velocities, relative to the model, depending on the position of the model during the measurement. Positive vertical velocities relative to the model are in the direction from keel to deck while horizontal velocities are toward the starboard side of the model. Thus, half-plane two-dimensional velocity data, collected for each of the four rotations of the model/wake generator, can be resolved by appropriate addition, subtraction, and/or trigonometric relations to provide three-dimensional velocity data at each point.

### 2.3.3 Steady Velocity Measurements: Nominal Wake

The impeller RPM of the tunnel(which controls tunnel volumetric flow and hence water speed in the test section) was set to 221, an arbitrary operating point within the comfortable working range of the facility. With a dummy hub mounted on the model in place of the model propeller, velocities in the test section varied only spatially with respect to the model. Measurements of this time invariant *nominal wake* due to the presence of the model/wake generator were possible. Detailed nominal wake surveys at six axial locations(stations) were then conducted: three stations upstream of the propeller and three stations downstream of the propeller. The locations of the six stations are shown in Figure 2-9.

Two-component velocity data were collected at points in the half-plane nearest to the laser. Sample locations were spaced at 5 degree intervals on semicircles at radii ranging from 9 to 135 mm from the propeller hub centerline, at intervals of 9 mm. Thus, there were 15 such semicircles for each of the six station locations (except where the inner radii fell within the model itself), with 37 sample positions on each semicircle. This sample pattern was repeated for each of the four model orientations. At each location a minimum of 300 two-component laser velocity readings was collected. The array of velocity values was then processed to determine the mean and standard deviation for each velocity component. The data collection program then discarded points which fell more than three standard deviations from the mean, and recomputed means and standard deviations from the reduced data set.

A new difficulty was identified as these data were being taken. Tunnel volumetric flow was monitored by a pair of pressure taps in the contraction section, and the LDV data processing system normalized the local velocity measurements by the velocities derived from the differential pressure (DP) readings. In this way, small changes in the tunnel volumetric flow(due, for example, to drift of the impeller motor) during the course of a data run could be accounted for. Systematic discrepancies of up to five percent were found between normalized velocities measured at the same point relative to the model when the model was in each of the four rotational orientations.

The explanation for the discrepancies was that the relationship between DP read-

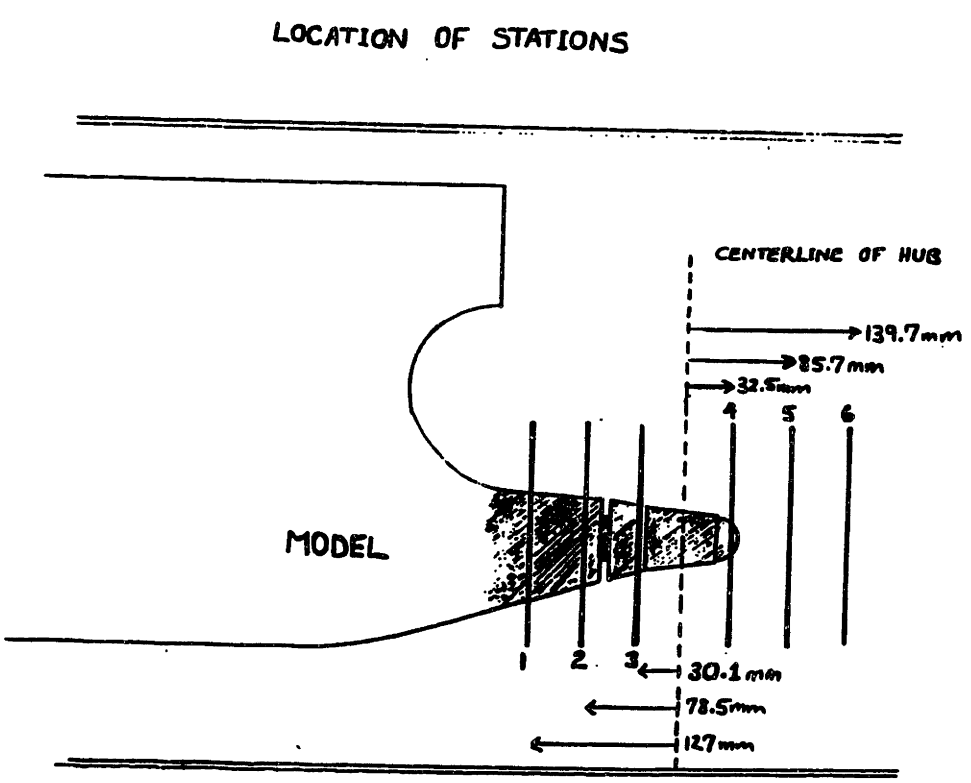


Figure 2-9: Station Locations

ing and tunnel volumetric flow was affected by the orientation of the model. The bow of the model extended part way into the contraction section, and since the bow was not axisymmetric, the flow near the pressure taps was slightly different for each orientation. It was therefore necessary to develop a different calibration factor for each of the four orientations of the model to allow measurements from the four rotations to be directly compared. This procedure was successful in yielding consistent data from each of the four model orientations. For each station, velocity data from each orientation was combined and duplicate data was averaged.(See Appendix A for a more detailed account of the calibration and conglomeration process). Contour plots of axial velocity and cross-flow vector plots were generated and are shown in Figures 2-10 through 2-21. A consistent pattern is evident as the wake evolves in the axial direction.

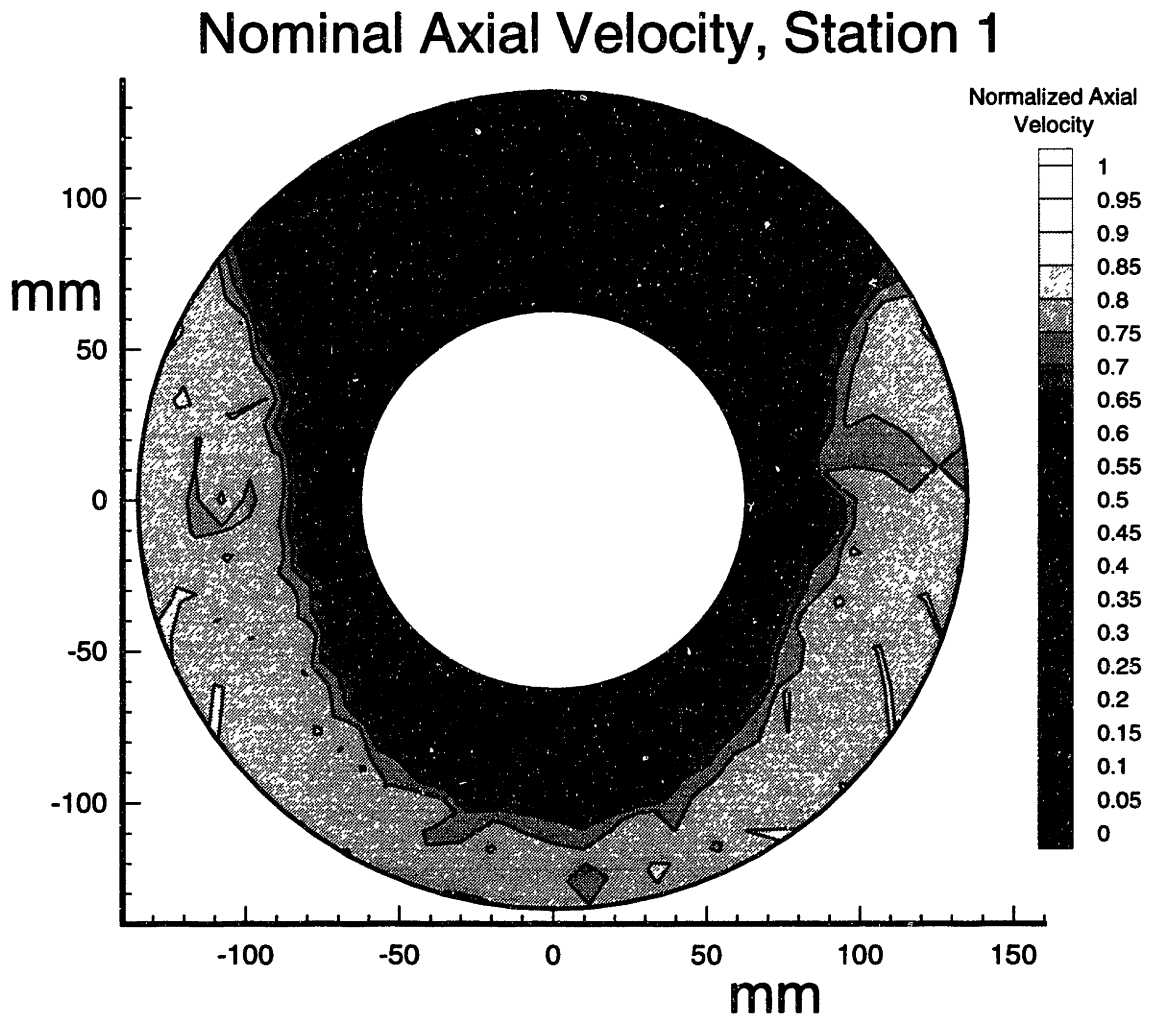


Figure 2-10: Measured nominal axial wake, Station 1

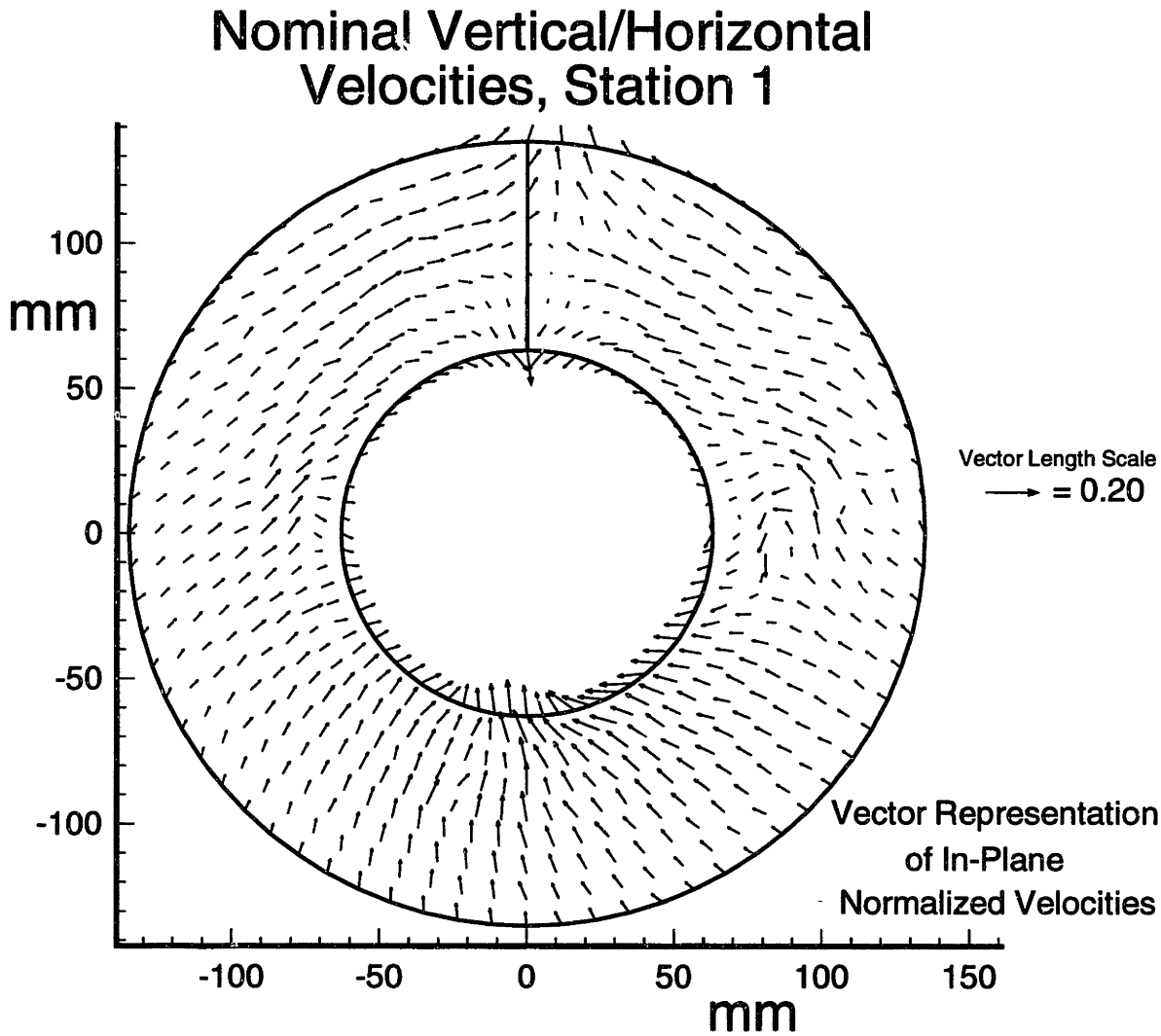


Figure 2-11: Measured nominal horizontal/vertical wake, Station 1

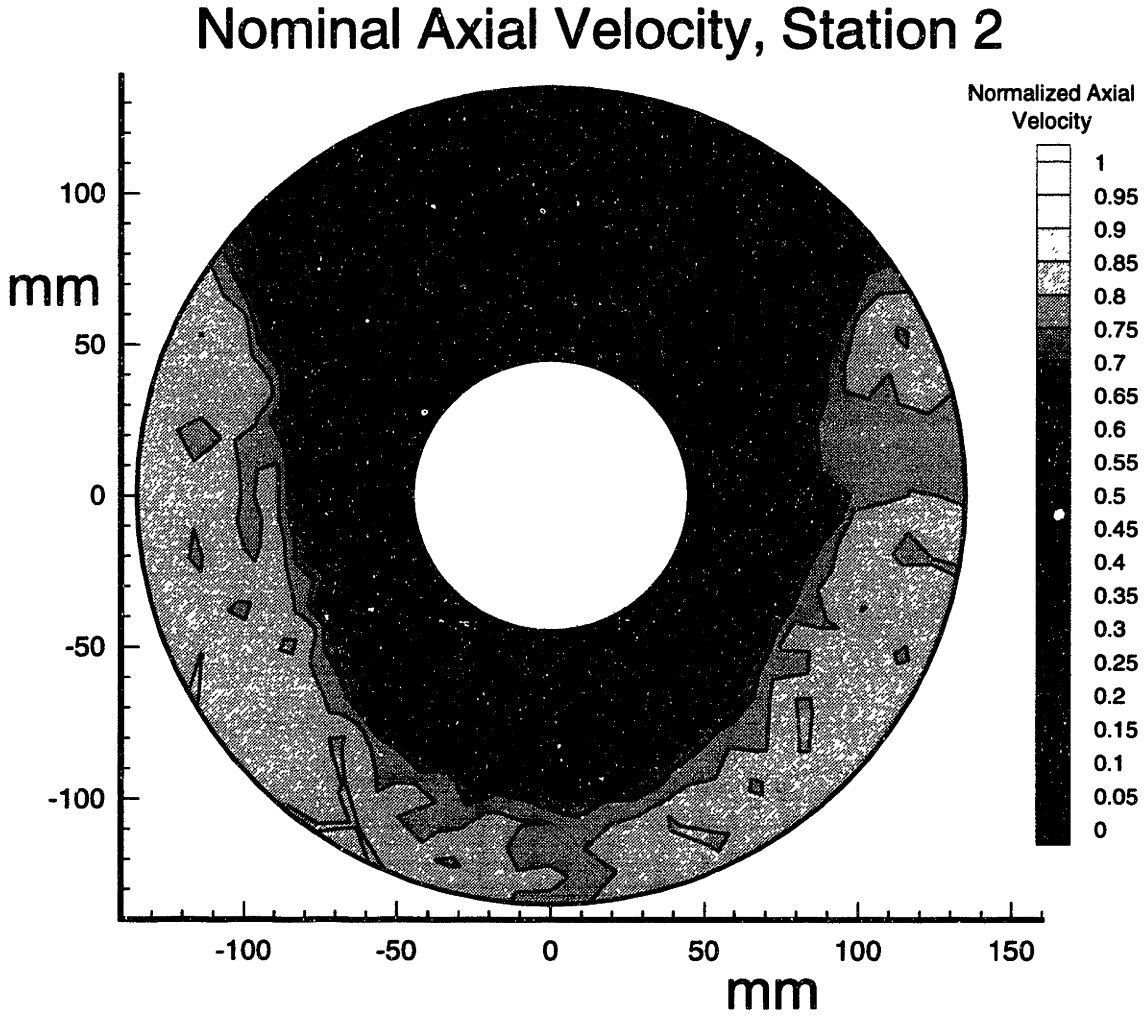


Figure 2-12: Measured nominal axial wake, Station 2

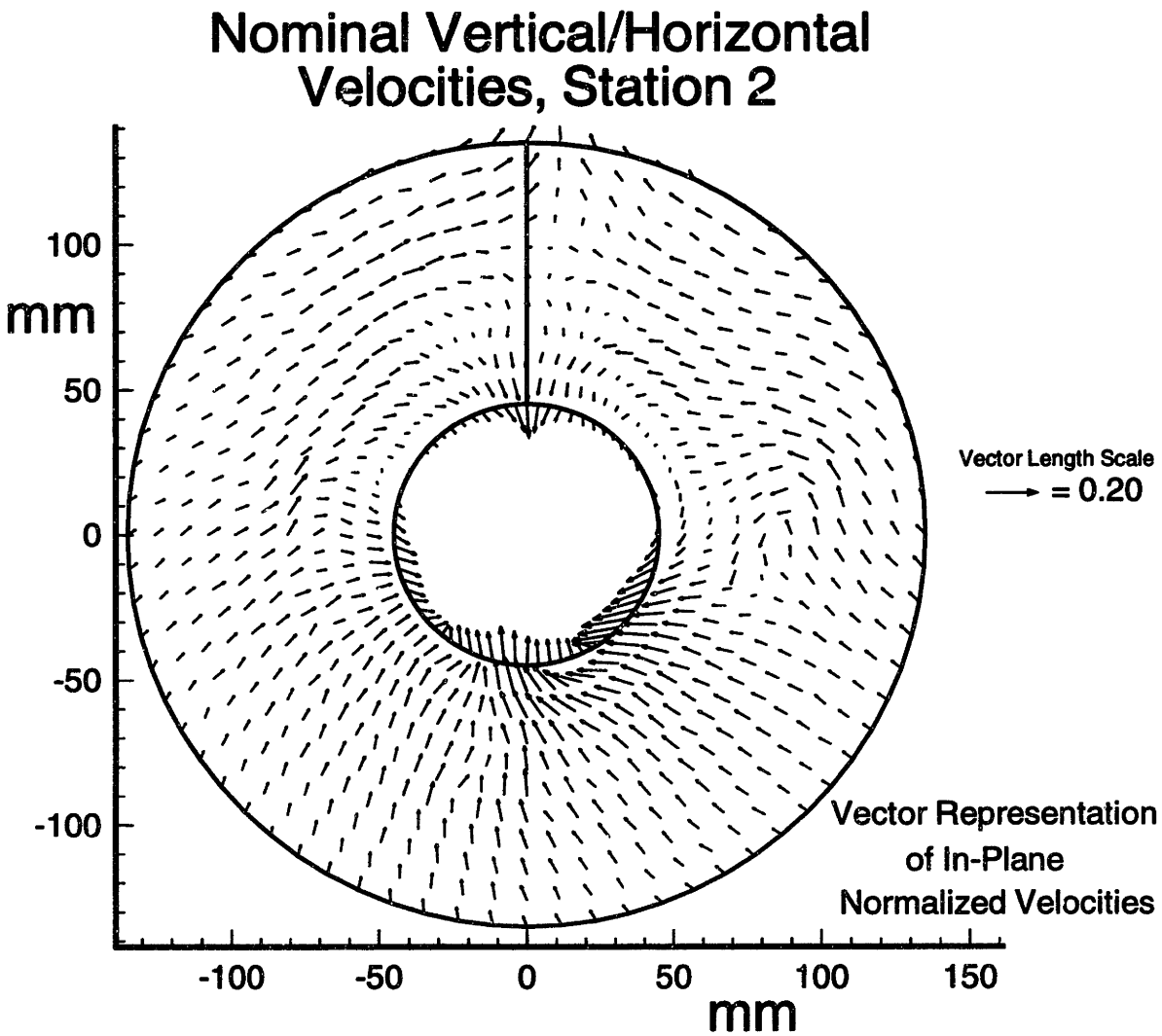


Figure 2-13: Measured nominal horizontal/vertical wake, Station 2

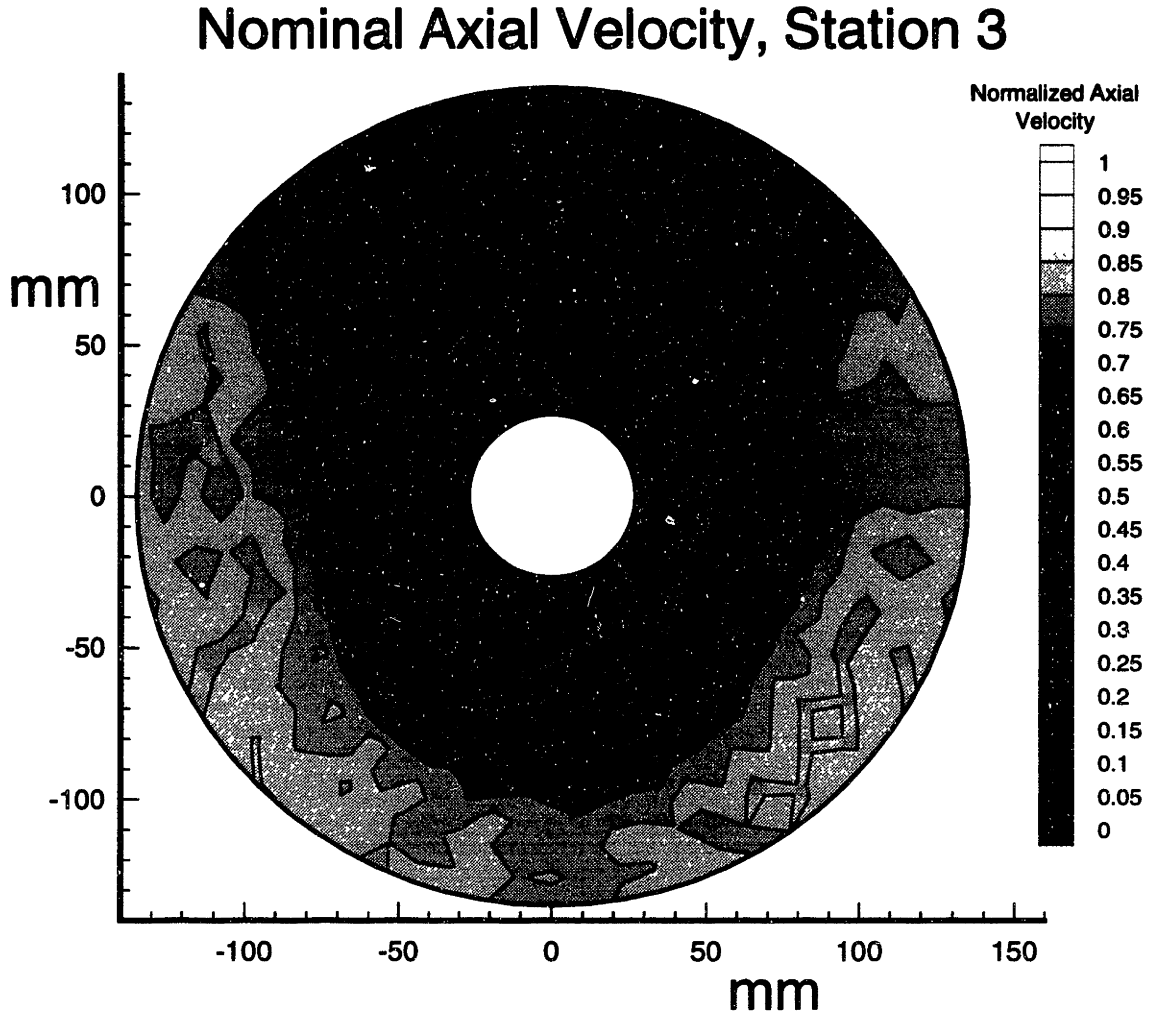


Figure 2-14: Measured nominal axial wake, Station 3

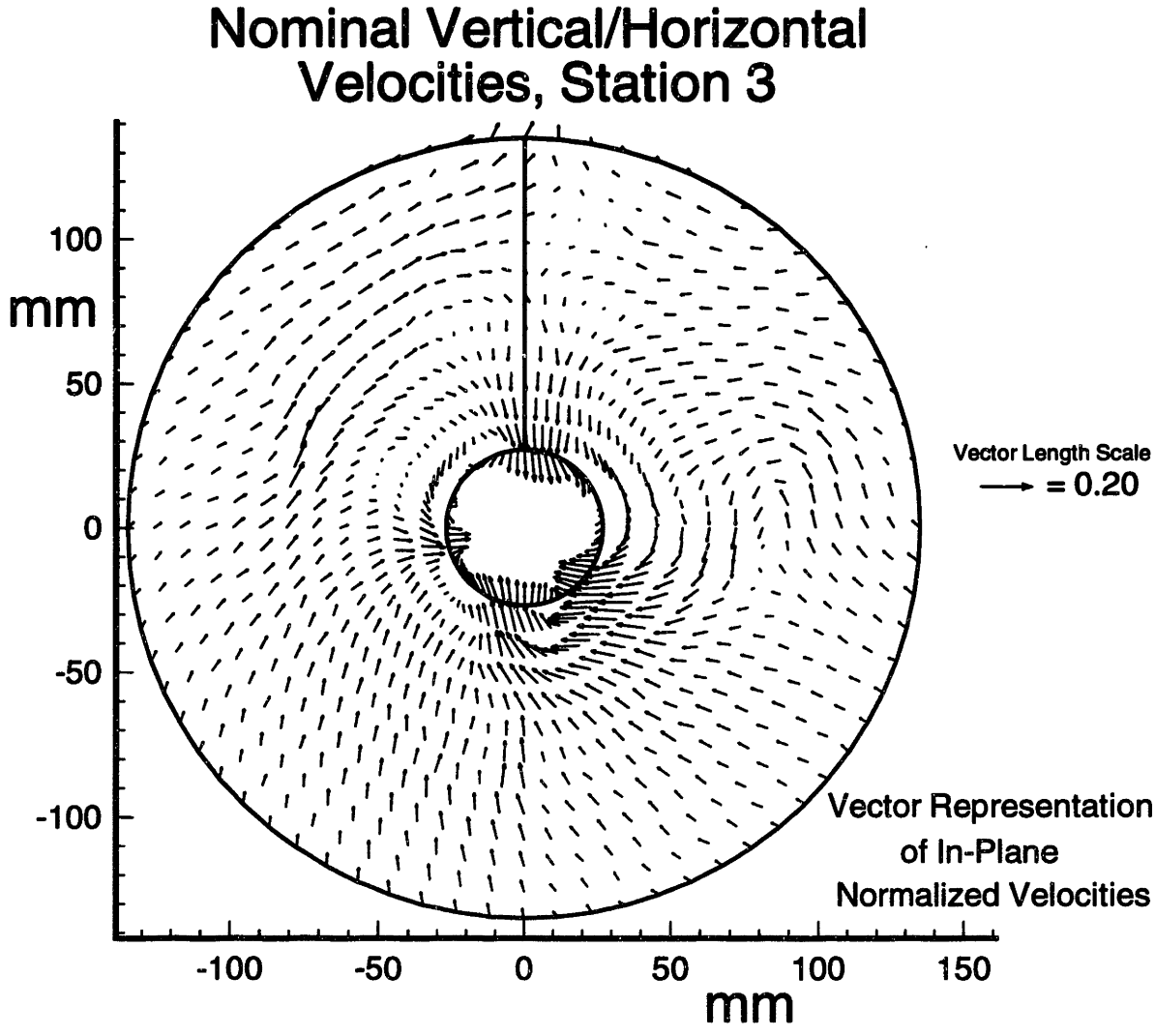


Figure 2-15: Measured nominal horizontal/vertical wake, Station 3

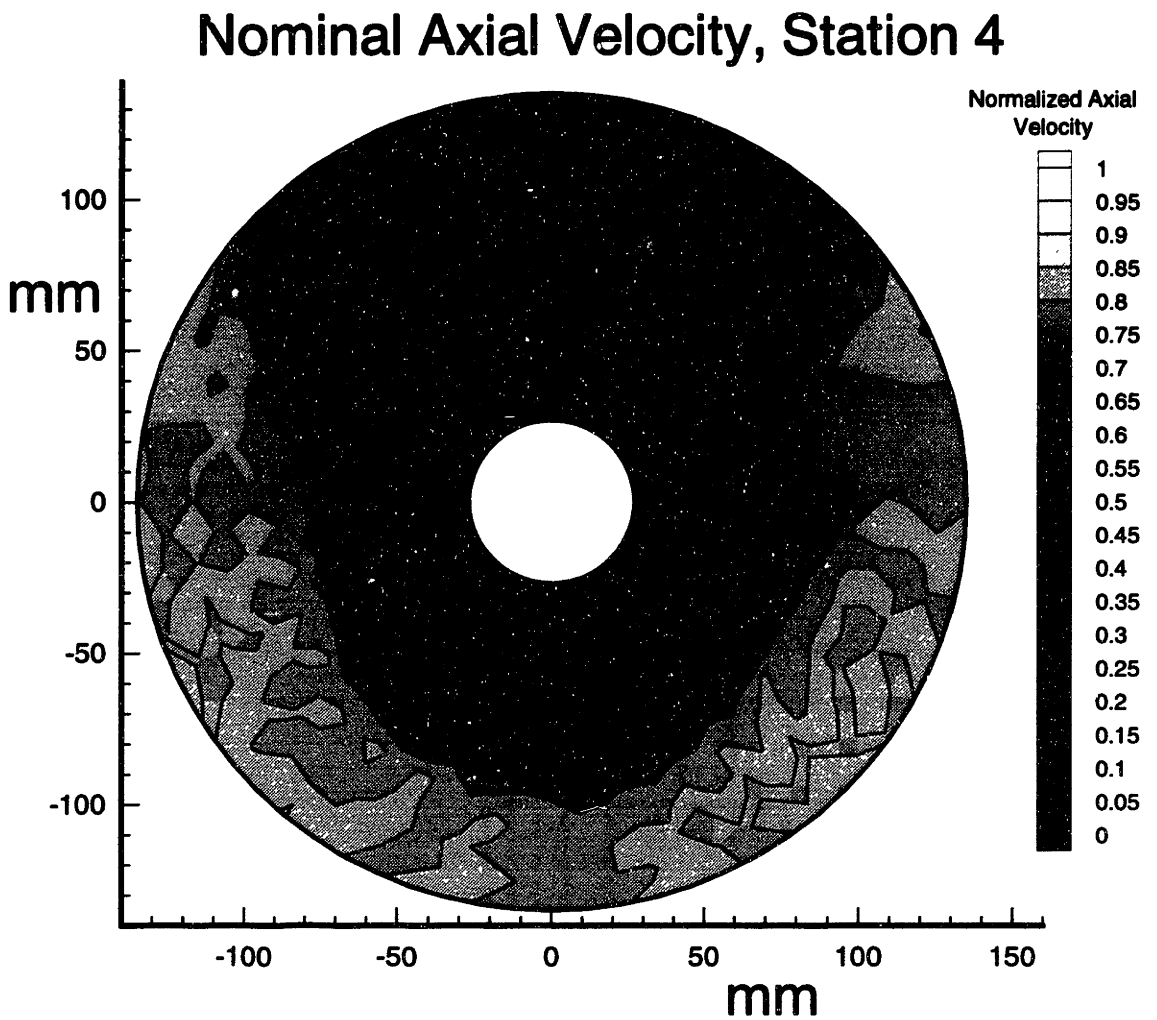


Figure 2-16: Measured nominal axial wake, Station 4

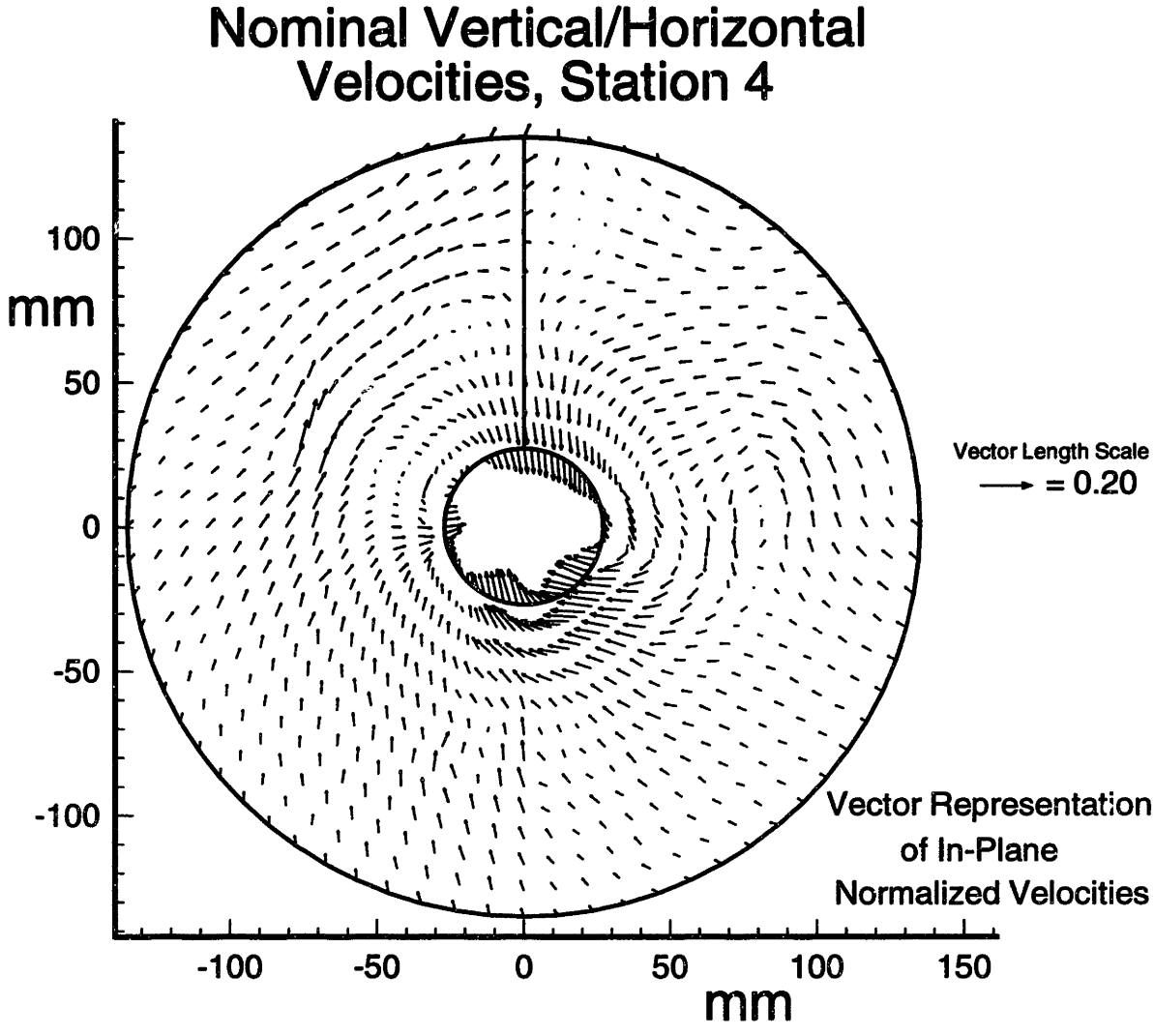


Figure 2-17: Measured nominal horizontal/vertical wake, Station 4

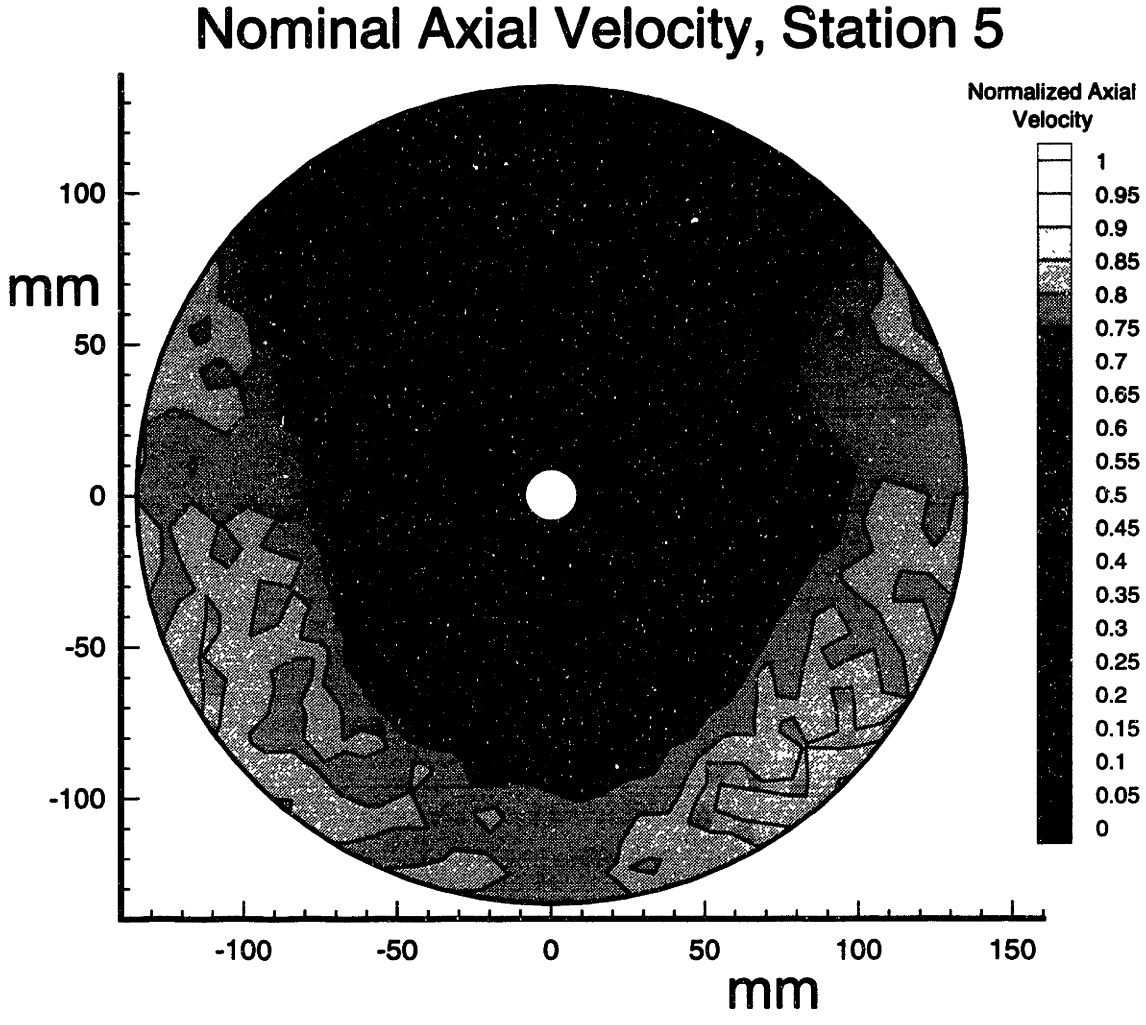


Figure 2-18: Measured nominal axial wake, Station 5

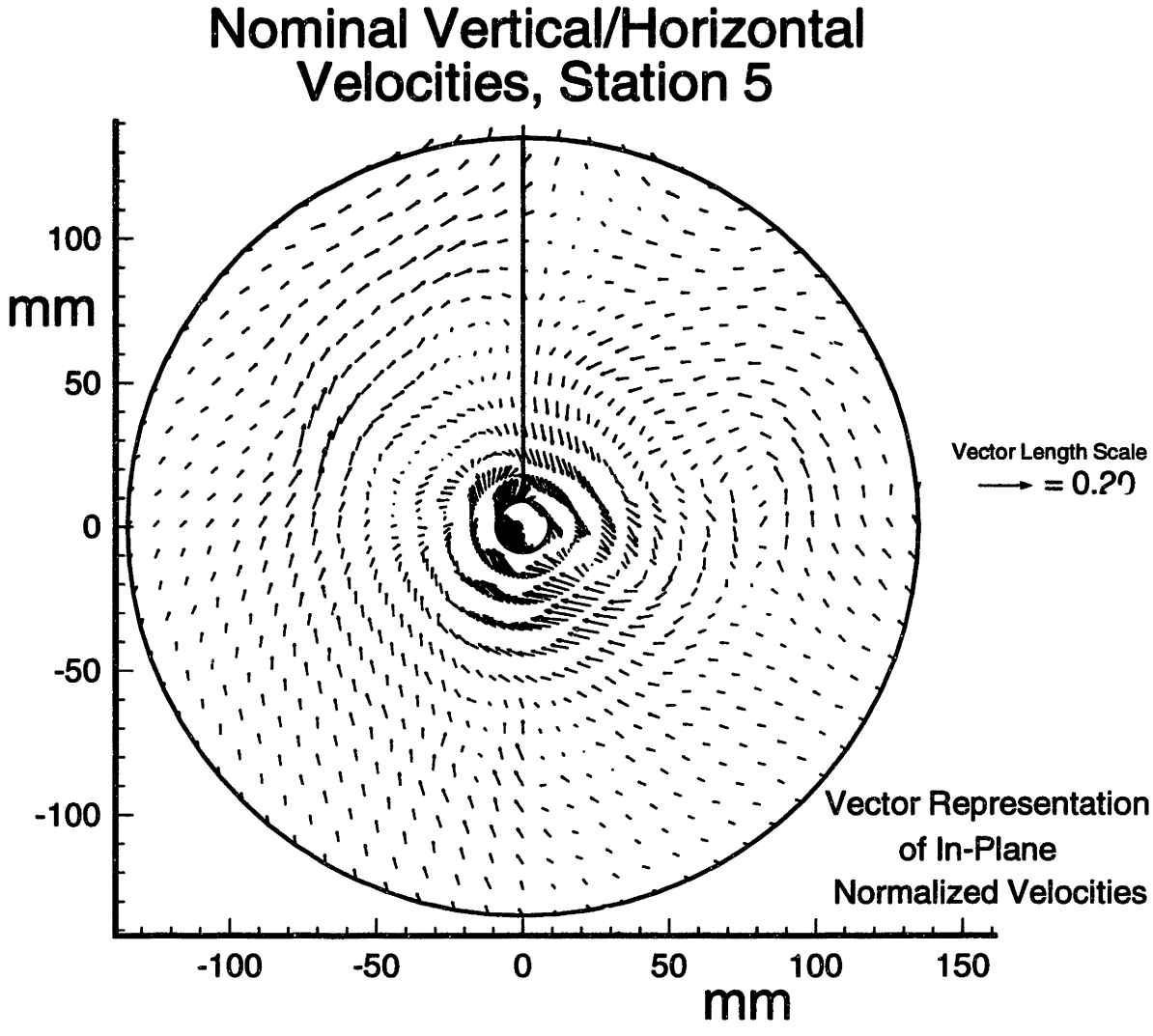


Figure 2-19: Measured nominal horizontal/vertical wake, Station 5

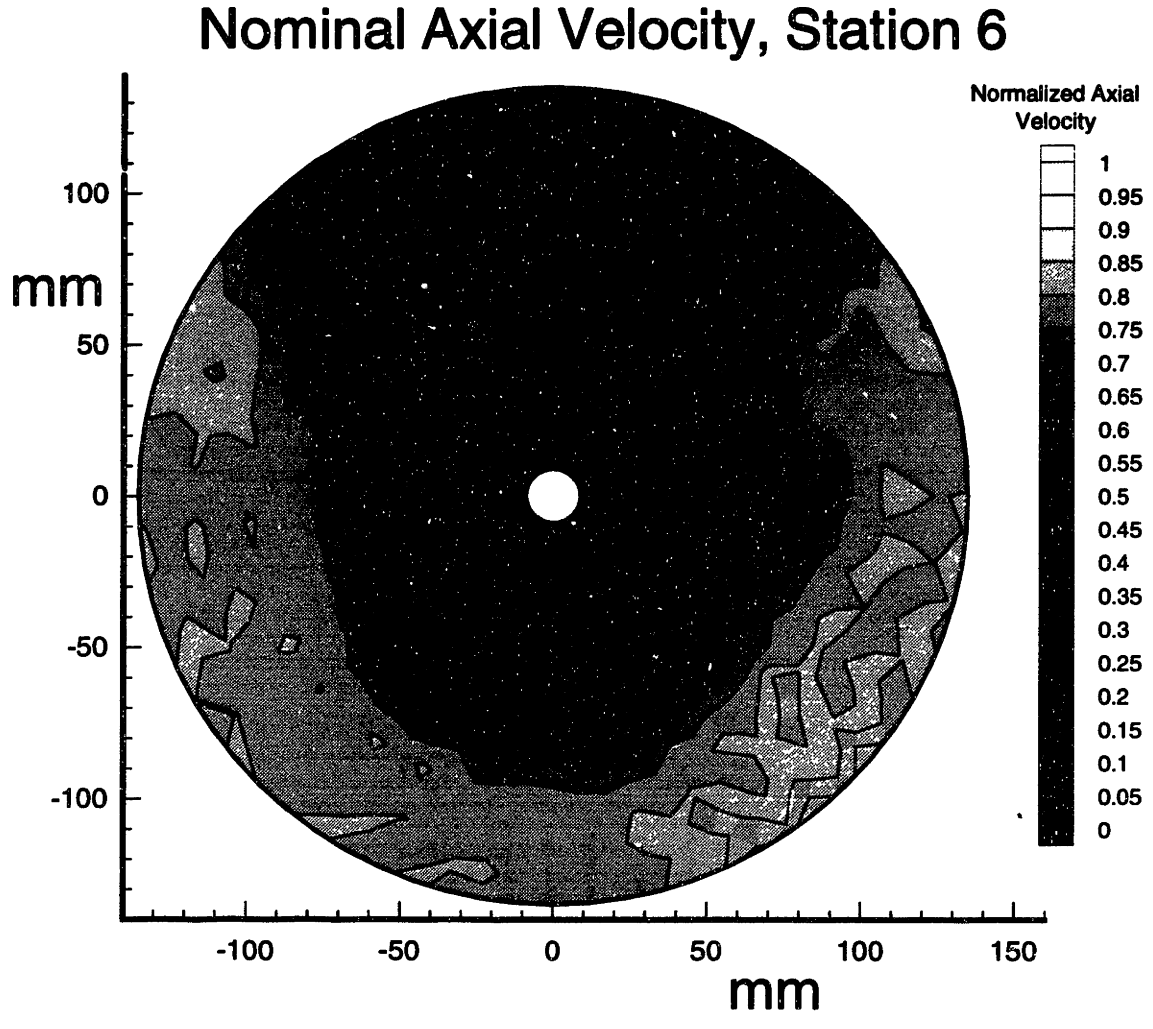


Figure 2-20: Measured nominal axial wake, Station 6

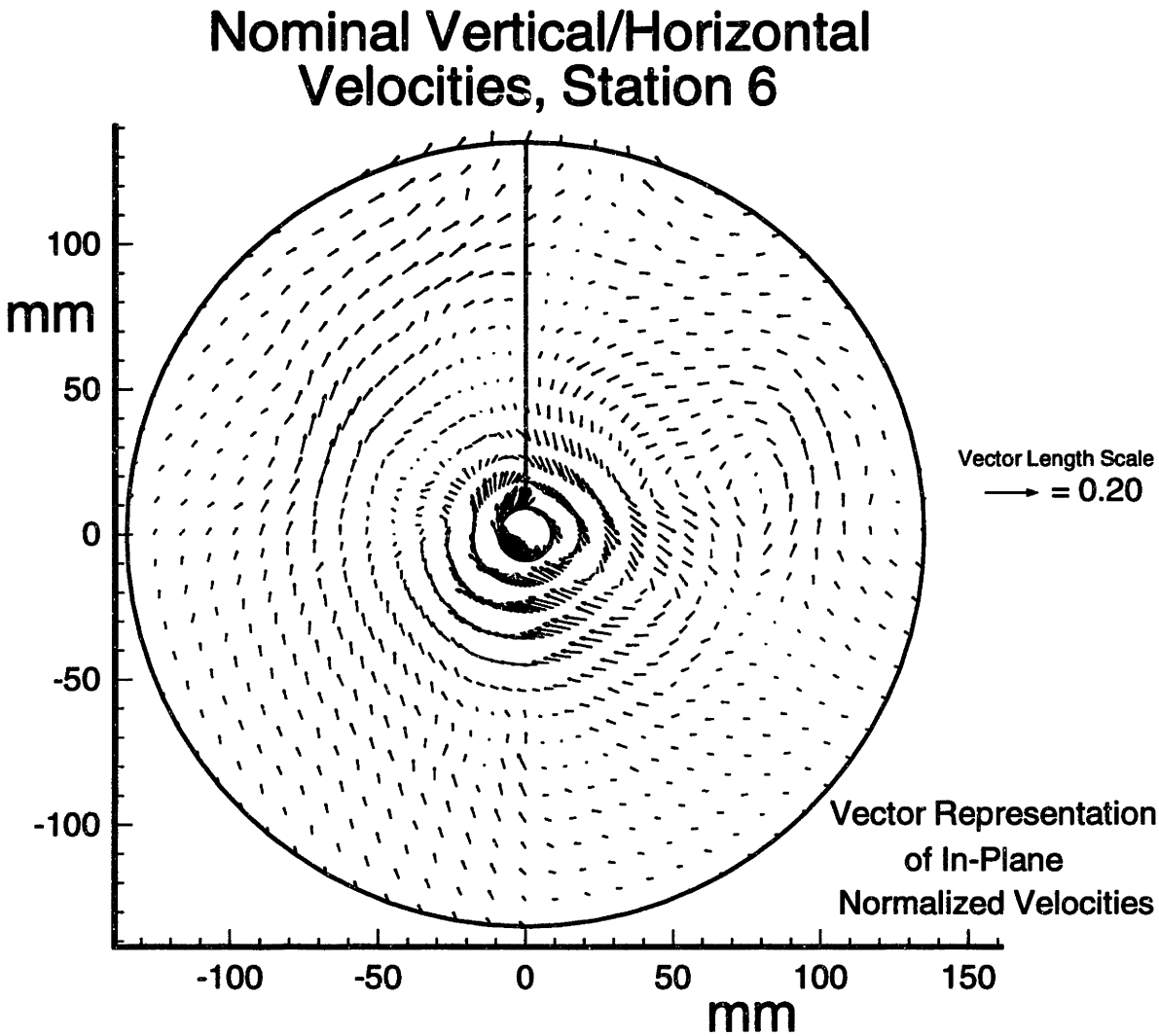


Figure 2-21: Measured nominal horizontal/vertical wake, Station 6

## 2.4 Determination of Total Wake

### 2.4.1 Unsteady Velocity Measurements: Total Wake

A test was performed with the model propeller in operation behind the underbody model. With the tunnel impeller RPM set to 221, as it was for the nominal velocity measurements, it was found that a propeller RPM of 1302 allowed the model propeller design thrust coefficient, $K_T = 0.209$, to be matched.

At stations 1 and 3, measurements were taken of the *total wake*, the wake which varies spatially *and* temporally due to the combined effects of the model/wake generator and the operation of the model propeller.

At station 1, approximately 0.6 propeller diameters upstream of the plane of the operating propeller, preliminary measurements were taken which confirmed the expectation of a negligible time-varying portion of the total wake that far upstream. Thus, total wake data for station 1 was taken in the same manner as the nominal/ steady wake data.

The axial location of station 3 was the closest the laser could be used, just upstream of the propeller, without the laser beams intersecting the spinning propeller. Station 3 was approximately 0.15 propeller diameters upstream of the plane of the propeller. As with the nominal wake data, two-dimensional velocity measurements were performed in the half-plane closest to the laser and three-dimensional components were provided by combinations of data from the four rotations of the model. At each sample location, time varying LDV data was stored and averaged in 180 angular *bins*. These bins, determined by the output of a digital shaft encoder, allowed 2 degree resolution of the angular position of the propeller at the instant each particular velocity was sampled. Sample locations were spaced at 10 degree intervals on radii ranging from 32.4 mm to 108.17 mm (r/R=0.3 to r/R=1.0). For station 3, the 32.4 mm radius was the smallest radius at which sample points did not fall within the model. Data was also collected at 10 degree intervals at radii r/R=1.1 and r/R=1.2. At these radii, the time varying portion of the velocity components was small enough so that data was again taken in the steady format.

Mean total wake data from each of the four rotations of the model were then combined and averaged for stations 1 and 3. Contour plots of the mean total axial velocities and cross-flow vector plots were constructed and are shown in Figures 2-22 through 2-25.

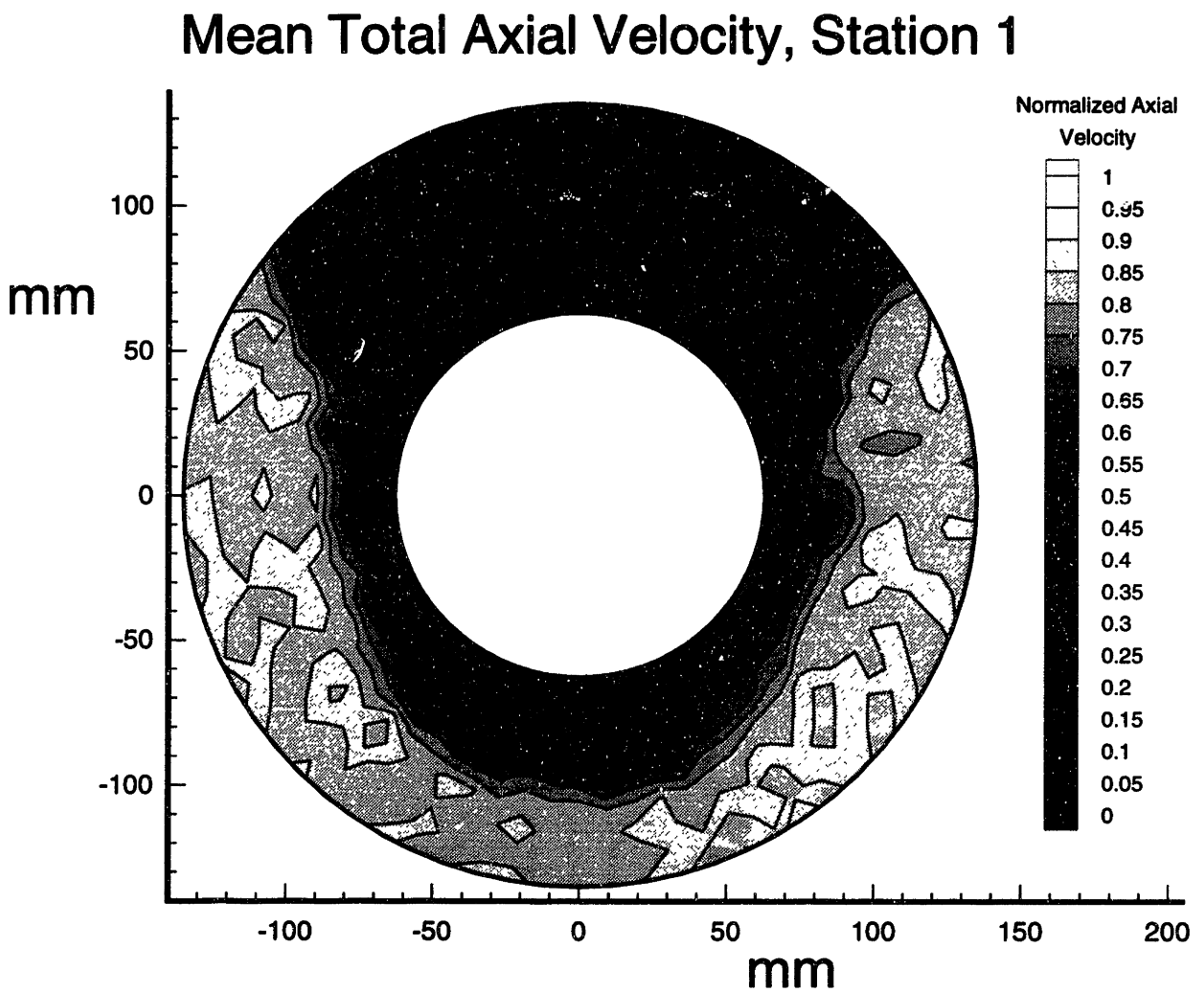


Figure 2-22: Measured total axial wake, Station 1

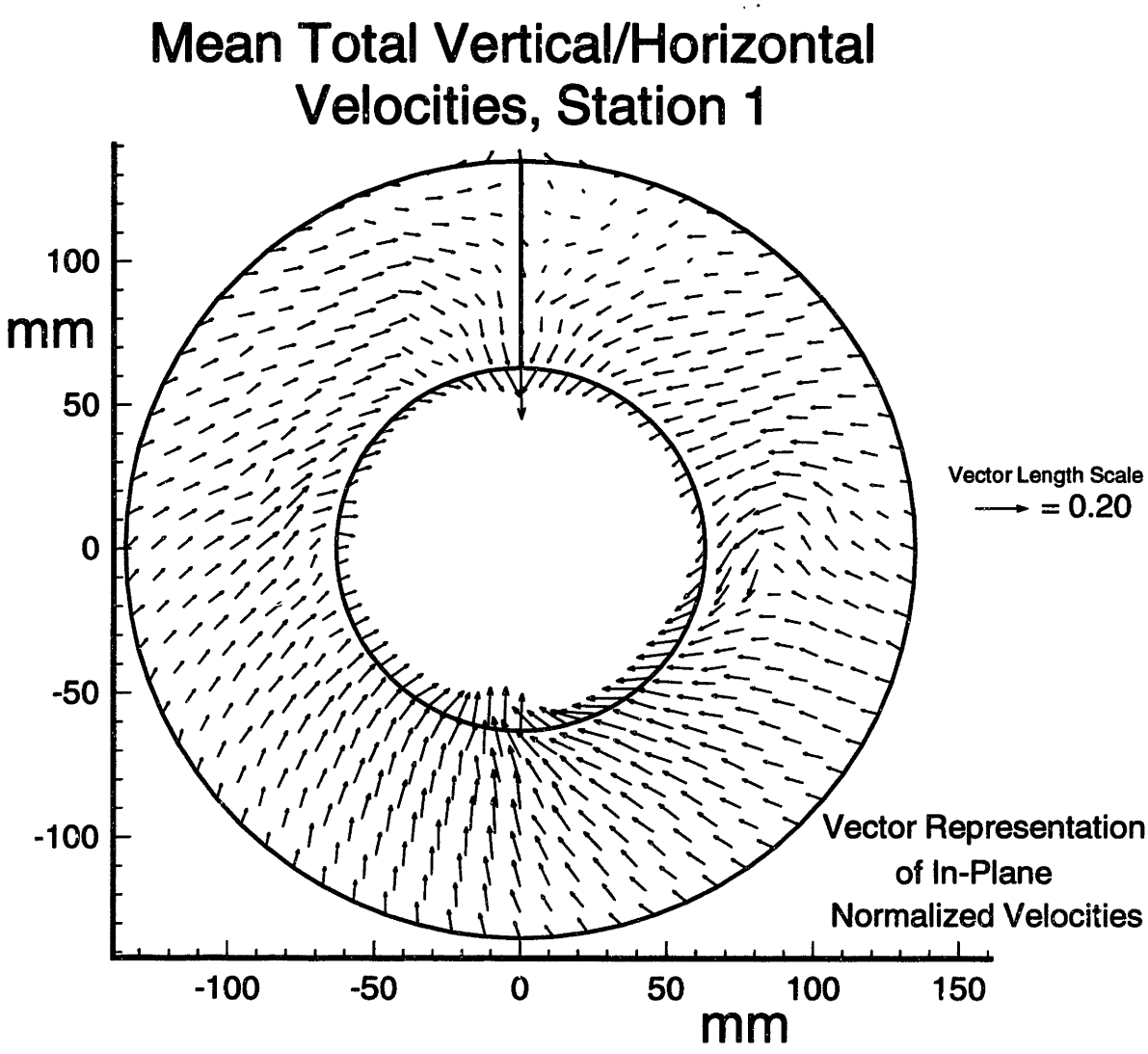


Figure 2-23: Measured total horizontal/vertical wake, Station 1

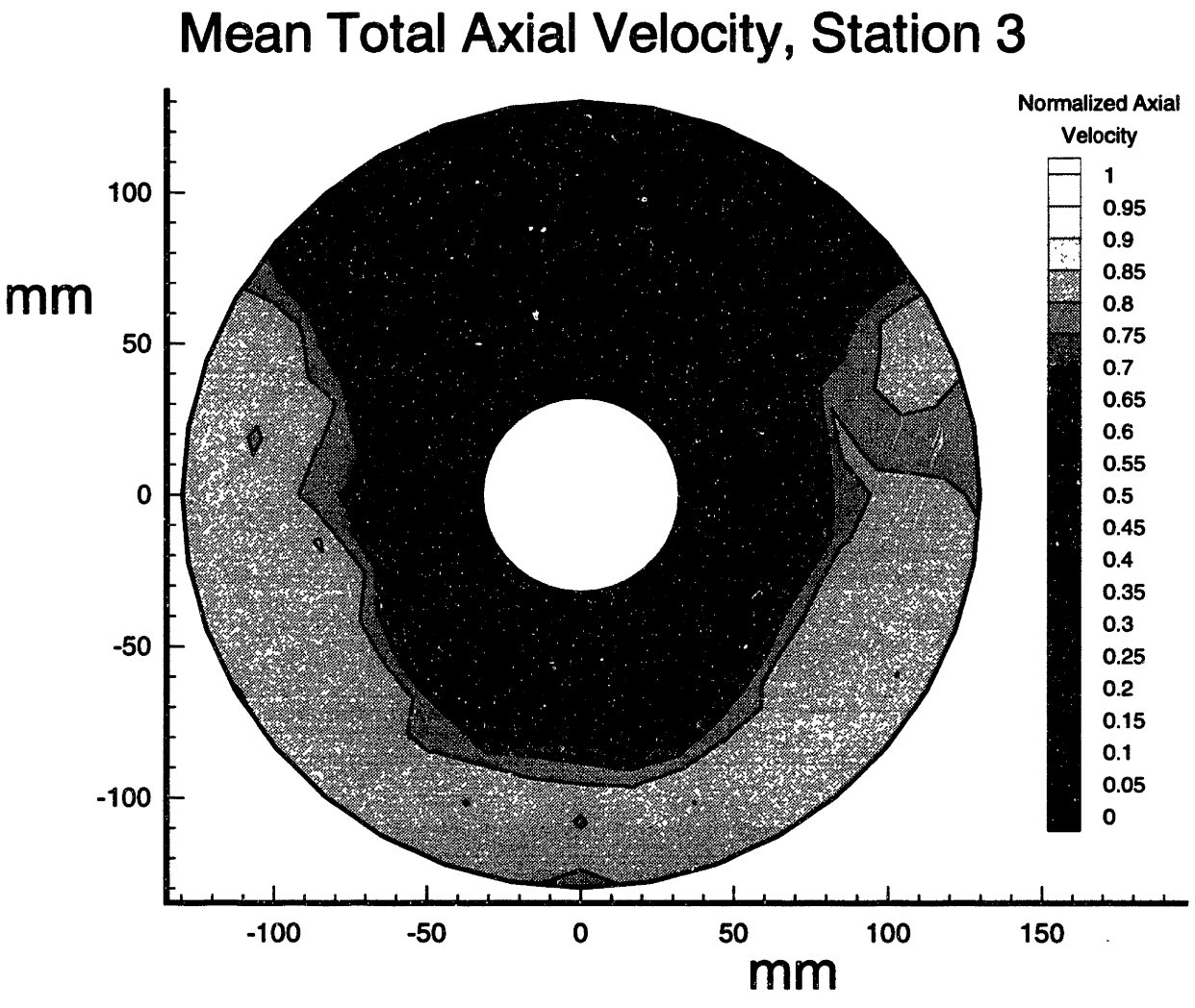


Figure 2-24: Measured total axial wake, Station 3

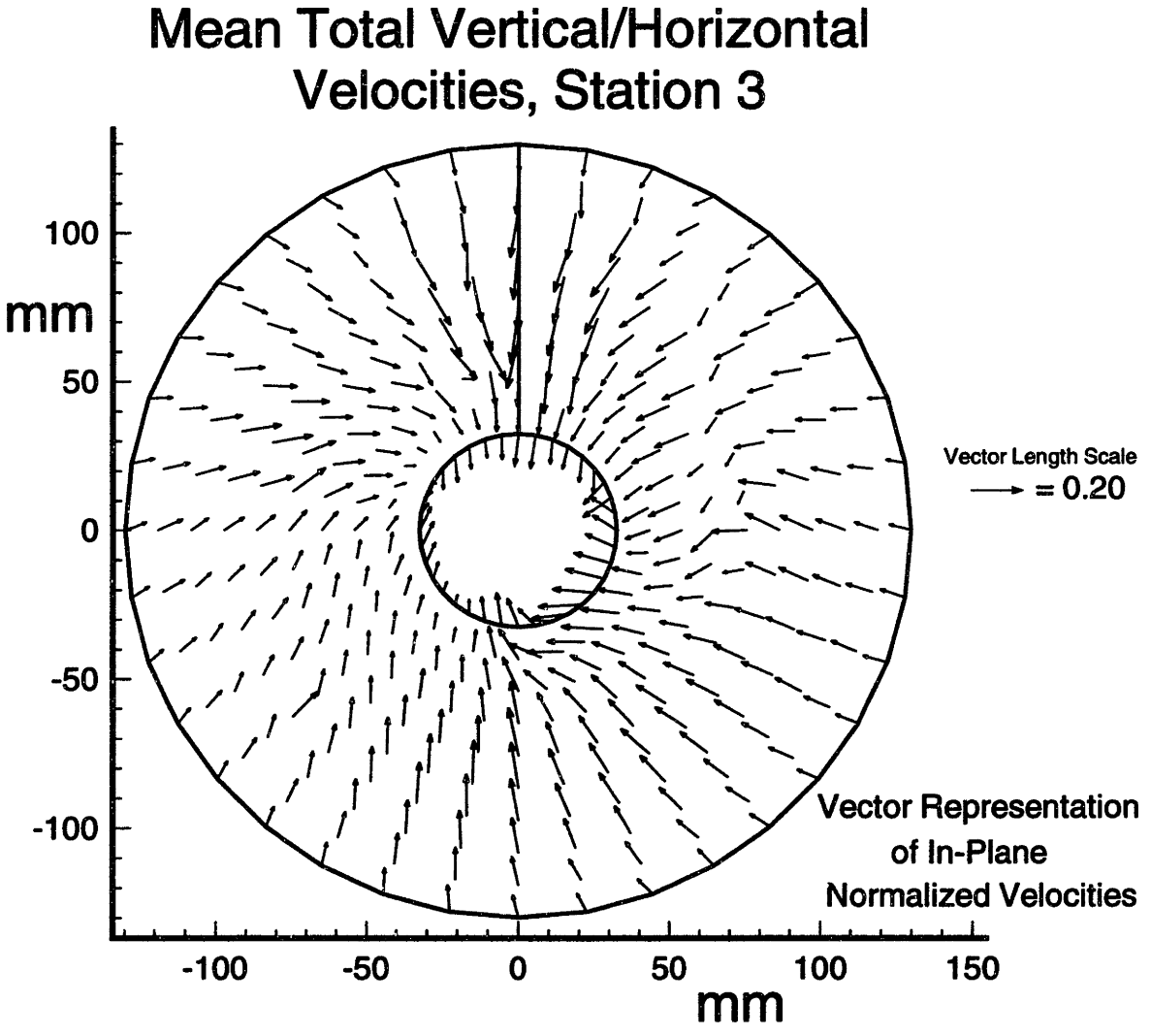


Figure 2-25: Measured total horizontal/vertical wake, Station 3

# Chapter 3

# Determination of Effective Wake

## 3.1 Theoretical Determination of Propeller Induced Velocities

A full scale propeller geometry file was prepared and verified by plotting(See Figure 2-4 and Table C.1). The nominal axial wake velocities for station 3 were used as input to the MIT code *WAKEPROC*, which converted the velocities into harmonic coefficients(See Appendix B for the Fortran code which prepares wake files for *WAKEPROC*). The design propeller advance coefficient, $J_A = 0.745$, and the design propeller thrust coefficient, $K_T = 0.209$,

$$
\begin{aligned}
(where\ J_A &= \frac{V_A}{(n \times D)} \\
K_T &= \frac{T}{(density \times n^2 \times D^4)} \\
V_A &= velocity\ of\ advance,\ feet\ per\ second \\
n &= propeller\ rotations\ per\ second \\
D &= propeller\ diameter,\ feet \\
T &= propeller\ thrust,\ lbs \\
density &= density\ of\ water, \frac{lbs}{sec^2 \times ft^4})
\end{aligned}
$$

were used along with the propeller geometry file and the nominal wake harmonics in the MIT code *PUF-2*.

*PUF-2* is a time-domain lifting surface code. The propeller geometry is represented by discrete vortex/source lattices which accomodate distributions of rake, skew, and pitch by locating the elements on the exact camber surface of each blade. Trailing vortex wake contraction and roll up and vortex sheet separation from the tips are accounted for. The procedure begins with the solution of a steady vortex system for the propeller operating in a ship wake consisting of the circumferential mean velocity at each radius. Once this is determined, the circumferential variations in the wake field are introduced and the steady-state oscillatory loading and vortex system develops in three or four revolutions of the propeller(See [4]).

Using the full scale propeller geometry, the nominal wake harmonic coefficients for station 3, and an arbitrary RPM of 100 as input to *PUF-2*, $J_A$ was varied until the calculated $K_T$ equalled 0.209, the design $K_T$ for the propeller. This manipulation of $J_A$ resulted, in effect, in the scaling up of all of the nominal wake velocities by a constant factor in order to provide operating conditions($J_A$, $K_T$) for the propeller that were very close to those for which the propeller was designed. This thrust identity occurred at $J_A$=0.741 (which compares well with the design $J_A$=0.745.).

Output from *PUF-2* representing the vortex system of the propeller as a function of propeller angular position was used as input to the MIT code *UFPV*. *UFPV* is an unsteady field point velocity code which predicts potential flow induced velocities, due to the operating propeller, at different axial, radial, and circumferential field points in the flow. *UFPV* calculates the combined induced velocities at a field point due to the strength of all of the vortices from the vortex system from the propeller. The output is given as induced velocities normalized on ship speed.

## 3.2 Determination of Model "Ship Speed"

As described in Chapter 2, individual LDV velocity measurements were normalized on DP readings of tunnel volumetric flow to account for any drift in the system during

each data run. The problem of the close proximity of the assymetric model and the DP taps was solved, allowing data taken when the model was at different orientations to be combined and compared directly. Blockage effects due to the model on the flow in the tunnel, though, made it difficult to determine a 'free stream' value for ship speed based on volumetric flow readings from the DP cells. Ship speed was necessary, as calculated induced velocities were obtained as values normalized on ship speed.

For conditions corresponding to the design $J_A$ and $K_T$, *PUF-2* calculated the Taylor wake fraction (1-w) to be 0.5426. Thus, for this arbitrary full scale trial,

$$V_{A,FS} = n \times D \times J_{A,FS} = \frac{100}{60} \times \frac{322.8}{12} \times 0.741 = 33.2215 \frac{ft}{sec} = 19.70 kts$$

and,

$$V_{S,FS} = \frac{V_{A,FS}}{(1-w)} = 61.23 \frac{ft}{sec} = 36.3 kts$$

Likewise to the above full scale trial, the model propeller was operated in the water tunnel at thrust identity ($K_t$=0.209). In order to convert from the arbitrary full scale ship speed ($V_{S,FS}$) to the tunnel operating conditions, tunnel ship speed was calculated as follows:

$$V_{S,TUN} = V_{S,FS} \times \frac{n_{TUN} \times D_{TUN}}{n_{FS} \times D_{FS}}$$

$$= 61.23 \frac{ft}{sec} \times \frac{1302 \times 8.517}{100 \times 322.8}$$

$$= 61.23 \frac{ft}{sec} \times 0.3435$$

Therefore,

$$V_{S,TUN} = 21.03 \frac{ft}{sec}$$

It was clear to us that these ship speeds were unrealistically high. This was attributed to the inconsistencies in this particular experiment between the velocities determined volumetrically by the DP cells and the actual flow velocities at the propeller, due to blockage effects by the model in the contraction section of the tunnel. This was not considered a problem, though, as LDV velocities were also normalized

on an unrealistically high free stream velocity as determined by the DP cells. The ship speed calculated above was used likewise as a normalizing factor for the theoretically determined induced velocities.

## 3.3 Verification of Induced Velocity Calculations

In order to check the induced velocity calculations, an arbitrary point at station 3 was used as the field point input to *UFPV*. The induced axial velocity at that location was calculated as binned data as a function of propeller position. The bins are 2 degrees wide, so 180 bins represents one rotation of the propeller. The experimental data for the total velocity measured at that location was plotted. Good comparison between the shape and magnitude of the calculated induced velocites and the measured total velocity was apparent, as shown in Figure 3-1.

## 3.4 Calculation of Effective Wake

The total wake with the propeller in operation minus the propeller-induced velocity is considered the *effective wake*(See [7]). Comparison of the DP values on which the total velocity measurements and the nominal velocity measurments were normalized and the "ship speed" value calculated above on which the calculated induced velocities were normalized yielded a calibration factor(the same idea as those discussed in Appendix A) which allowed the direct subtraction of mean induced velocities from mean total velocities. Thus, mean values of the potential induced velocity were subtracted from the mean total velocity to give the mean effective velocities at stations 1 and 3.

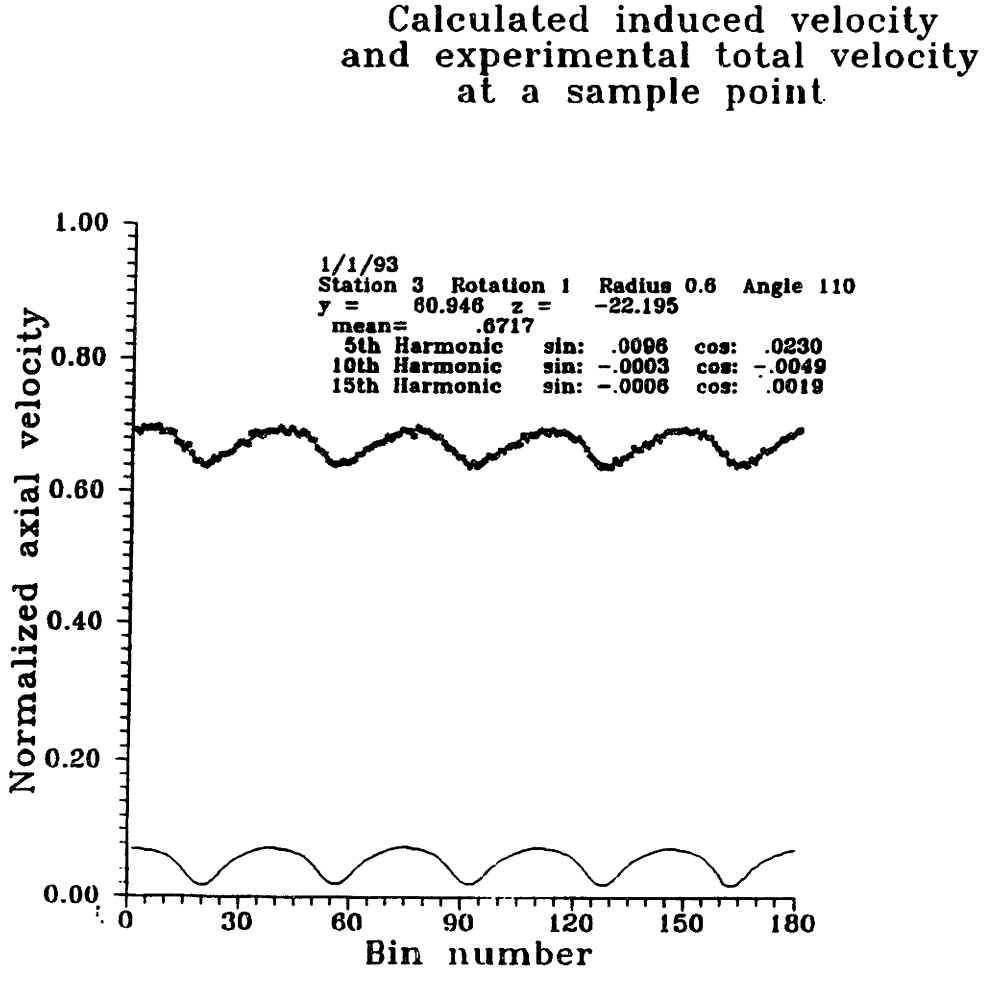


**Figure 3-1: Verification of Induced Velocities at a Sample Location**

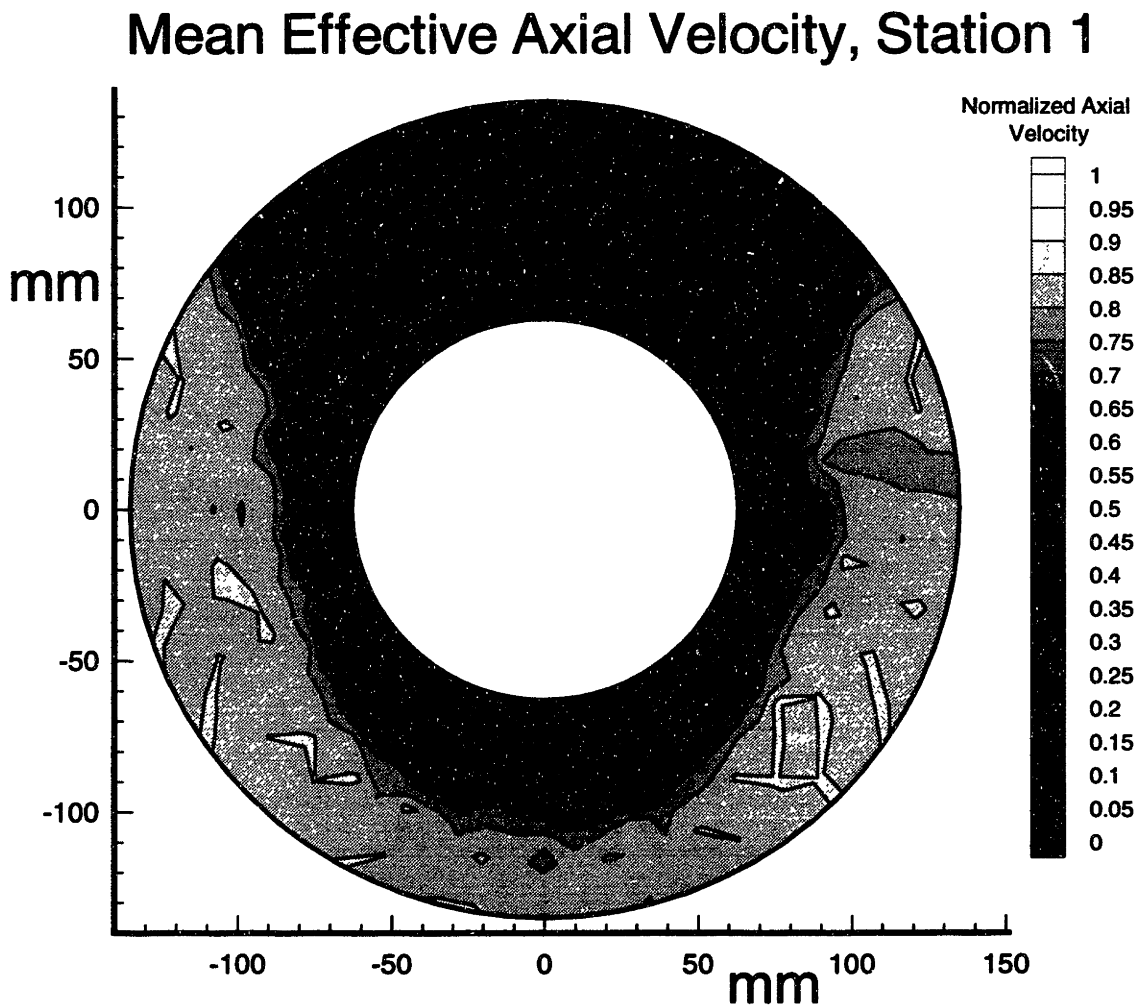


Figure 3-2: Measured effective axial wake at Station 1

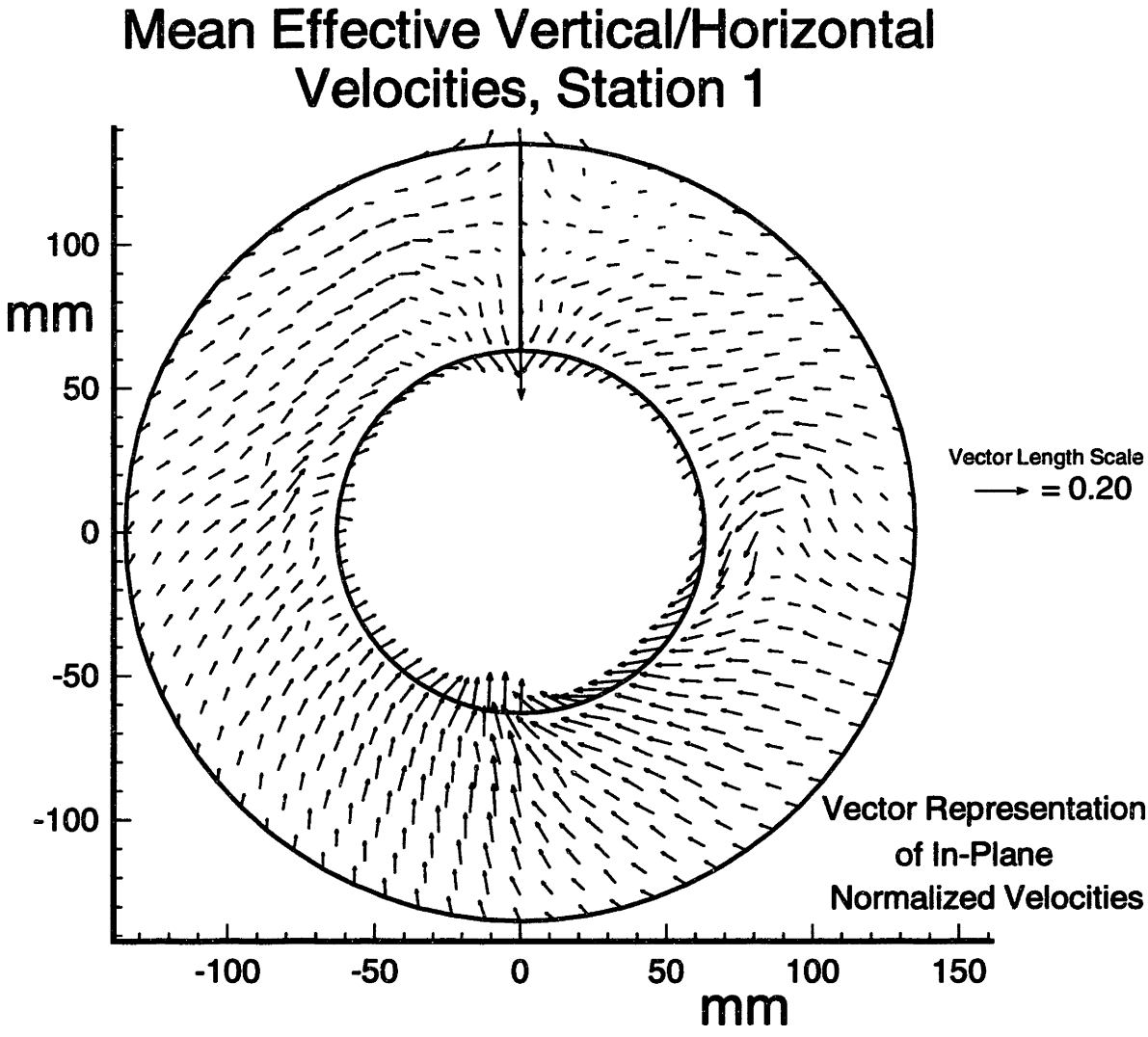


Figure 3-3: Measured effective horizontal/vertical wake at Station 1

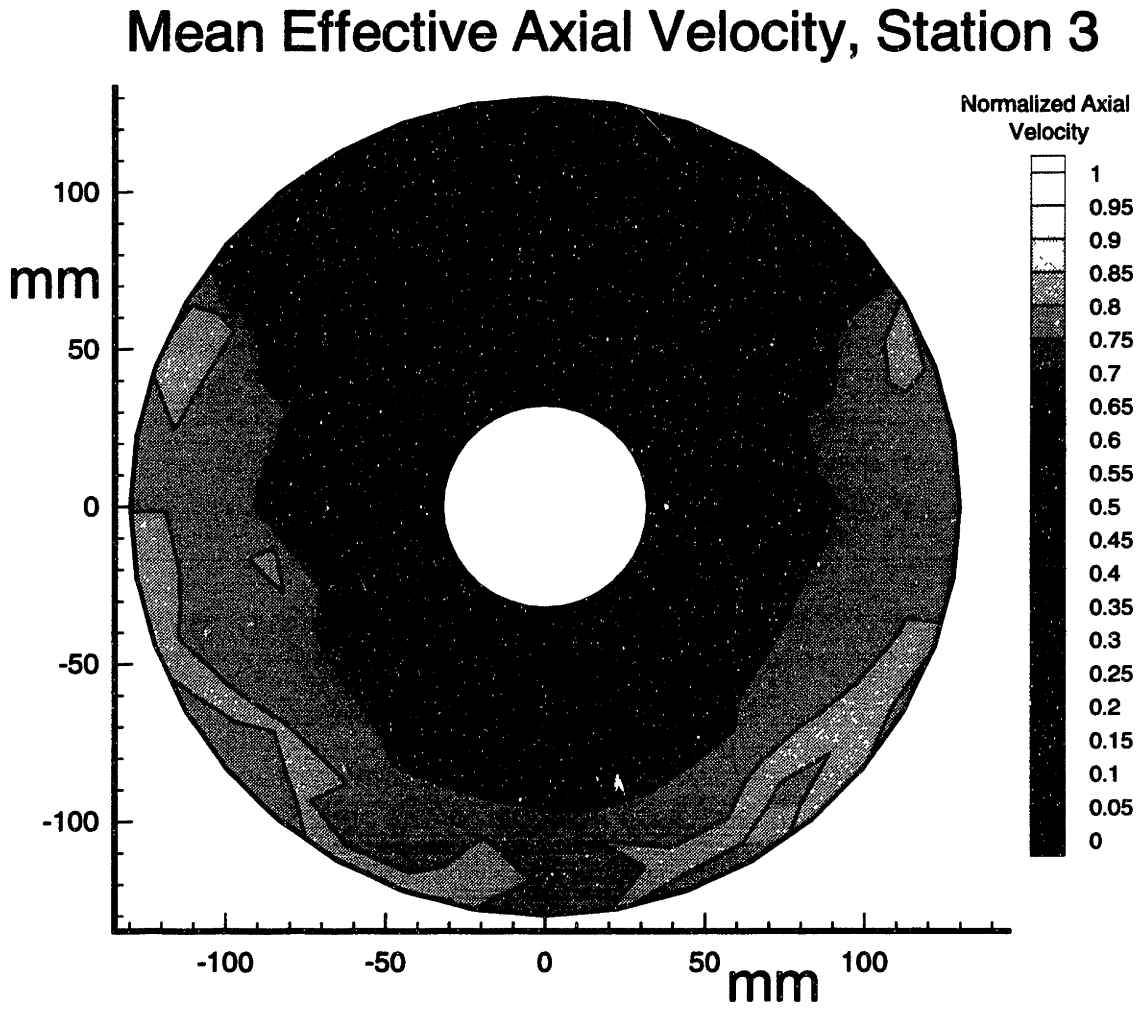


Figure 3-4: Measured effective axial wake at Station 3

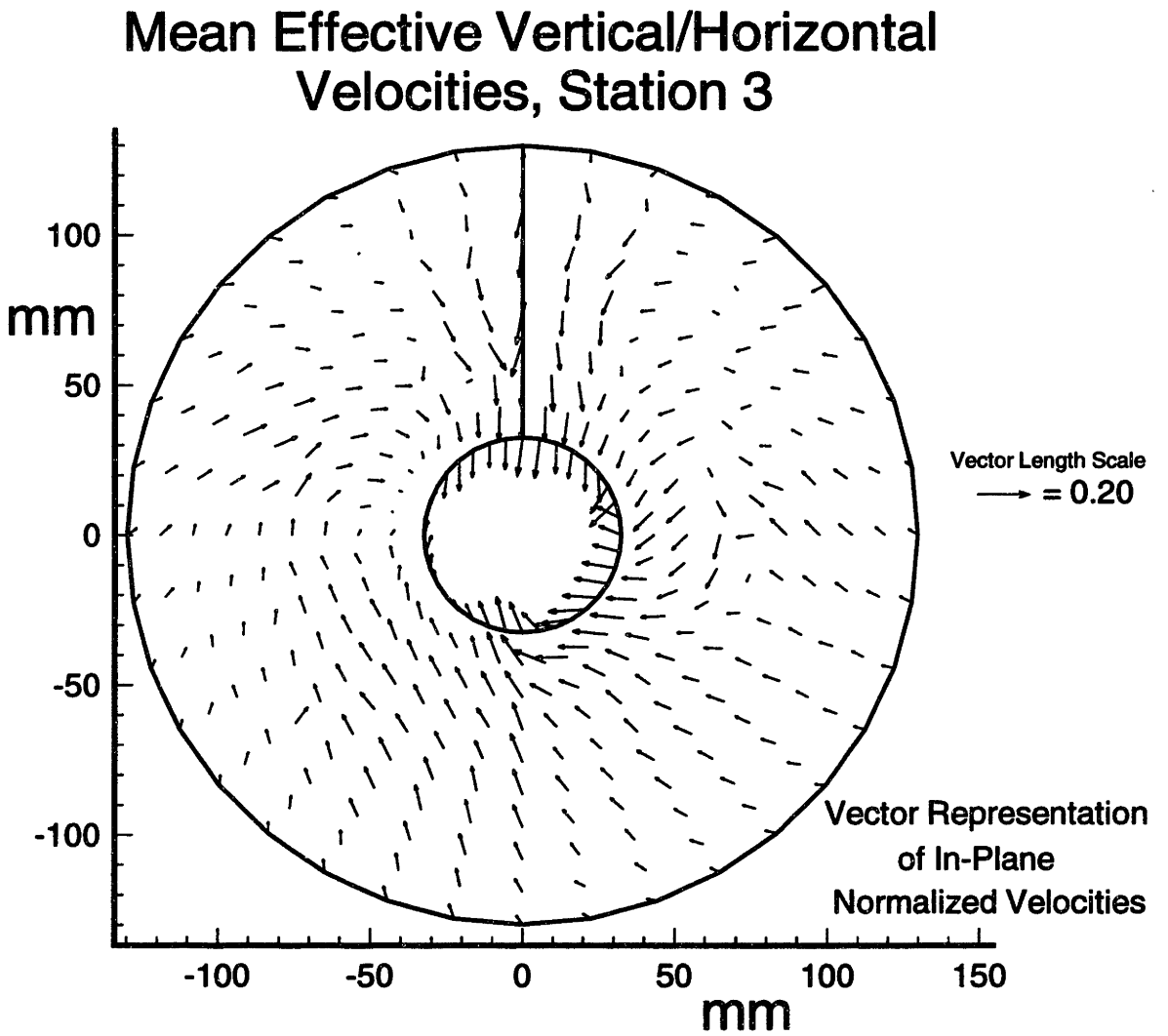


Figure 3-5: Measured effective horizontal/vertical wake at Station 3

## 3.5 Comparison of Nominal, Effective, and Total Wakes

Circumferential averages of the axial velocities, as functions of the radius, were prepared for the station 1 nominal, effective, and total wakes. These averages were then plotted as shown in Figure 3-6.

At large radial distances from the propeller axis, the magnitude of the propeller induced velocities were expected to go to zero(See [7]). Were this the case, the effective wake would have been equal to the nominal wake at those points. From Figure 3-6, the circumferential average effective axial velocities were greater than the circumferential average nominal axial velocities for *all* experimental radial locations. Though it is typical for the effective axial velocities to be different (greater) than the nominal axial velocities for the inner radii, differences between the two even as far from the propeller axis as r/R=1.25 must have been caused by some characteristic of the experimental setup.

The difference between the circumferential average nominal and effective axial velocities at the outer radii was attributed to the close proximity of the tunnel walls. Due to the action of a propeller, there is increased fluid volume flow through the propeller disc and therefore axial velocities of an fluid tend to increase as the fluid approaches the propeller. Due to continuity, streamlines(stream surfaces in 3-D) are thus shifted inward toward the axis of the propeller. Due to the presence of the tunnel walls, though, there existed a physical limit on the portions of the flow from which extra fluid could be drawn. The restriction caused by the tunnel walls disallowed ample fluid to be drawn radially into the contraction and resulted rather in a general axial acceleration of the cross-section of the upstream axial flow.

The elimination of the difference between the nominal and effective axial velocities at the outer radii was accomplished by scaling down the total wake axial velocities by a constant percentage across all radii. The percentage chosen was that which decreased the circumferential average total velocities enough so that when the calculated propeller induced velocities were subtracted from this new total wake (creating

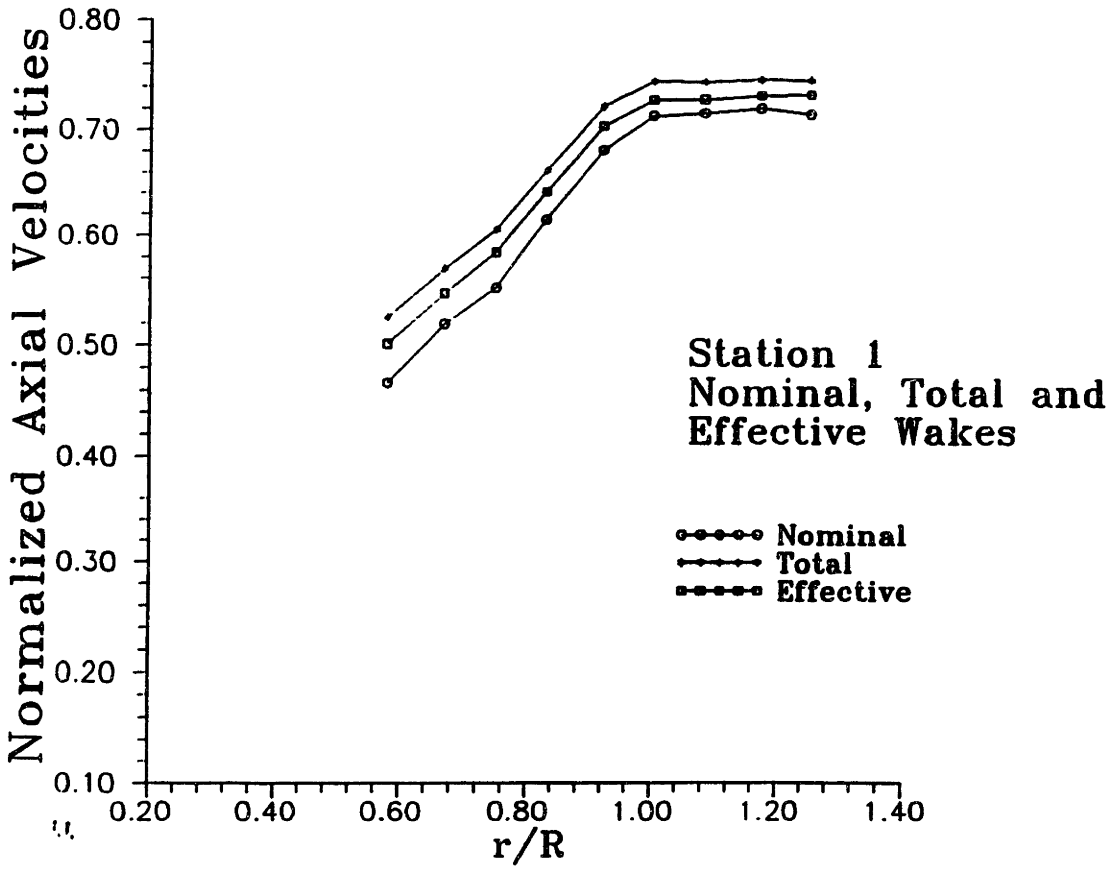


**Figure 3-6: Circumferential Averages of Axial Velocities at Station 1**

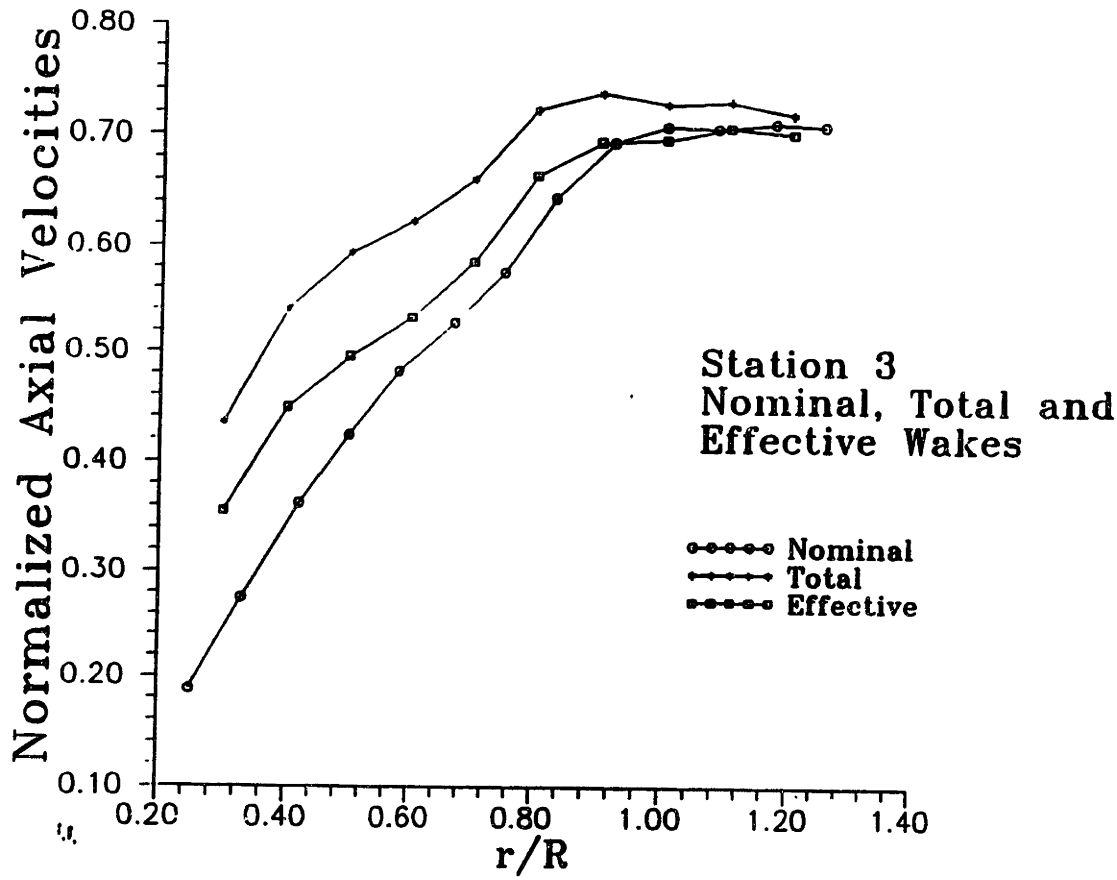


**Figure 3-7: Circumferential Averages of Axial Velocities at Station 3**

a new effective wake), the circumferential average effective axial velocities at the outer radii were roughly equal to the corresponding velocities from the nominal wake. The actual percentage decrease of the total velocities was 1.9%. The magnitude of the decrease of the total velocities was greater for the outer radii, as the outer radii velocities were larger than the inner radii velocities. The circumferential average axial nominal, effective, and total wakes are shown in Figures 3-8 and 3-9 after the 1.9% scaling down of the total wake.

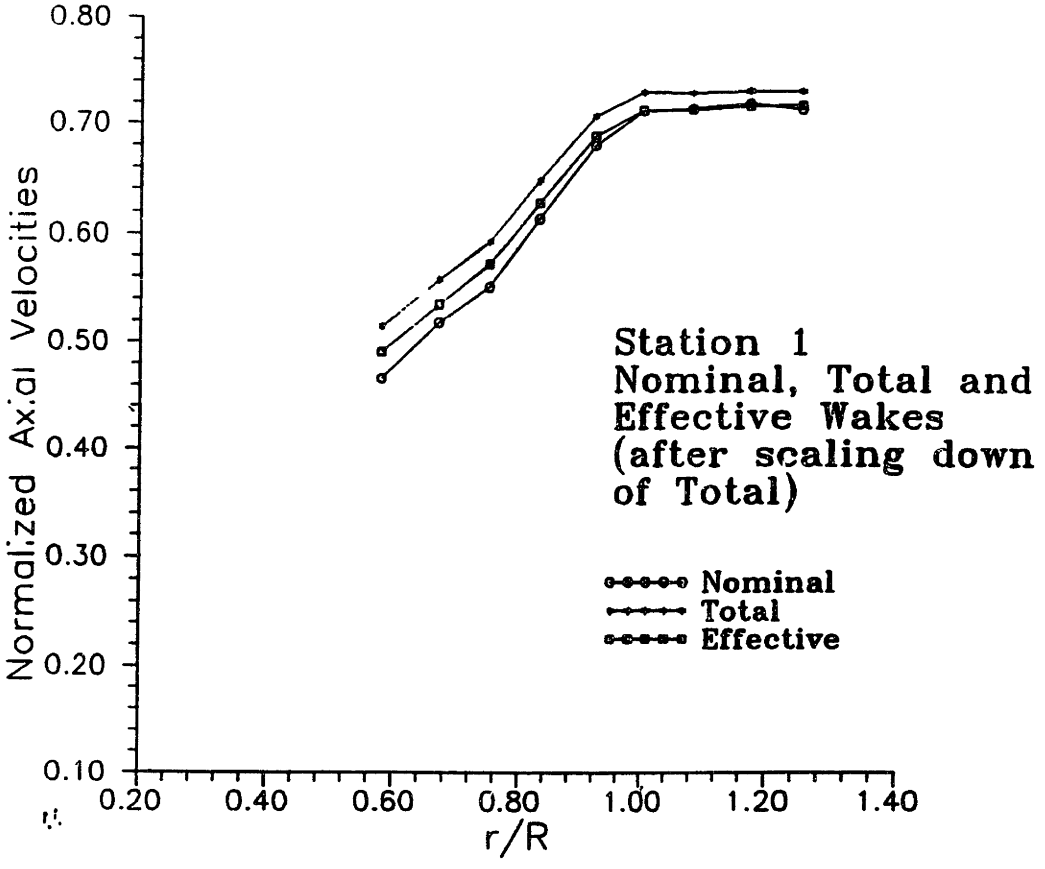


**Figure 3-8: Adjusted Circumferential Averages of Axial Velocities at Station 1**

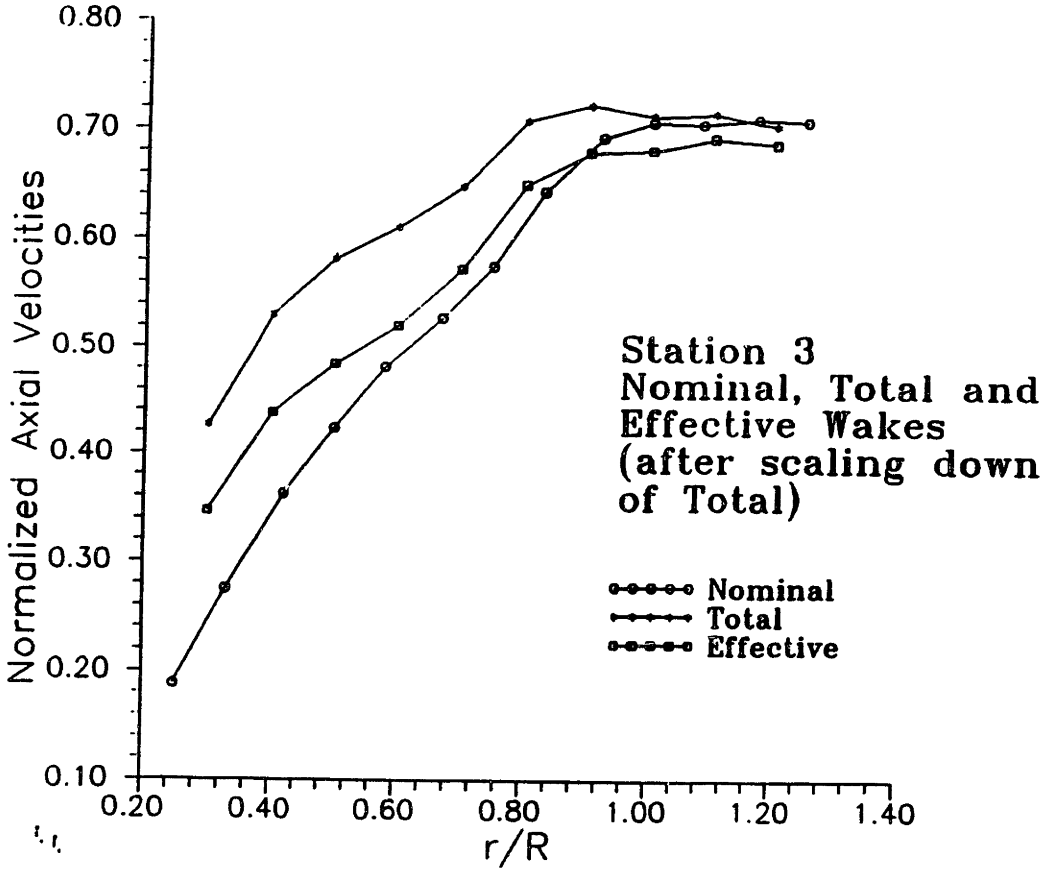


**Figure 3-9: Adjusted Circumferential Averages of Axial Velocities at Station 3**

# Chapter 4

# Conclusions

Past investigations in this area of marine propeller design have concentrated on representation of the effective wake as circumferential averages and/or for axisymmetric bodies. The work presented here succeeds in representation of the model scale nominal, total, and effective wakes as functions of both radial and circumferential position for a flow field representative of a typical surface vessel. Consistent patterns were evident as each wake evolved in the axial direction.

A comparison was made between the calculated propeller induced velocities and the measured total wake velocities for an arbitrary experimental point. Good comparison between the shape and magnitude of the induced and total velocity fluctuations during a single revolution of the propeller was apparent. Continued research could explore the effectiveness of these induced velocity predictions as a function of location in the flow.

This research involved extensive detailed experimental work to map the three-dimensional nominal wake at three axial locations upstream of the propeller and three locations downstream of the propeller, as well as the total wake at two upstream axial locations. Total wake measurements taken approximately 0.6 propeller diameters upstream of the plane of the propeller indicated a negligible time-varying portion of the total wake this far upstream and beyond. Further work could detail the axial evolution of the three-dimensional total and effective wakes upstream of the operating propulsor. Also, with the large volume of experimental measurements of the

nominal and total wakes, and combined experimental and theoretical determination of the effective wake at several axial locations, the results of this research could be an effective means of assessing the performance of current theoretical methods which predict the effective wake for marine propellers.

# Appendix A

# The Calibration Process

## A.1 Combining Data From the Four Rotations

Due to the influence of the model's bow on the differential pressure(DP) cells, which monitor tunnel volumetric flow, each of the four rotations of the model resulted in normalized velocities(at the same location relative to the model) which differ systematically by as much as 5 percent depending on model orientation. For example, when the model was in the 270 degree rotation("keel" toward laser), the "deck" of the model was located very close to the DP taps in the tunnel, causing accelerated flow past the taps. This accelerated flow in the region of the DP taps had the result of making the tunnel recording equipment believe the flow in the tunnel was faster than it really was. Therefore, with nothing changed in the experimental setup(namely the impeller speed which governs water flow speeds in the tunnel) except for the orientation of the model, the assymetry near the bow of the model caused normalized velocity measurements, taken at the same point relative to the model, to be different for different model rotations. These changes resulted in normalized velocities from different model orientations which could not be directly compared.

As stated in the main text, the purpose of the DP cell readings used as normalizing velocities was to account for any possible drift in tunnel nominal flow rates during the course of a given data collection session and also from day to day. It was found, though, that the tunnel settings drifted very slowly, allowing the operator ample

opportunity to adjust the controls and maintain the system very close to steady state. The actual changes in tunnel nominal flow during a data run(and thus from day to day) were found to average around 3 or 4%. The result of this somewhat constant tunnel flow(and therefore somewhat constant DP reading) was that all of the normalized velocites taken for a particular rotation of the model were taken with a fairly constant normalizing factor. This allowed for the calculation of an average DP reading(the normalizing velocity) for each rotation by averaging the DP reading for all points in that rotation. This procedure was applied to both the nominal wake data and the total wake data. For example, the nominal wake average DP readings for each of the rotations at station #3 were as follows:

- 0 degrees - 18.98 $\frac{ft}{sec}$
- 90 degrees - 18.33 $\frac{ft}{sec}$
- 180 degrees - 19.12 $\frac{ft}{sec}$
- 270 degrees - 19.74 $\frac{ft}{sec}$

Likewise, the total wake average DP reading for each of the rotations at station #3 were:

- 0 degrees - 19.48 $\frac{ft}{sec}$
- 90 degrees - 18.75 $\frac{ft}{sec}$
- 180 degrees - 19.53 $\frac{ft}{sec}$
- 270 degrees - 20.32 $\frac{ft}{sec}$

Note the different flow speeds for each rotation and also that the trends regarding which rotation is highest, lowest, etc. for the nominal wake also hold for the unsteady total wake. The reason for the higher flow speeds in general for the total wake is the "pumping" action of the operating propeller in the test section. Unlike the nominal wake study where a dummy hub was put in place of the propeller, the total wake portion of the testing took place with the model propeller spinning: the spinning

propeller, providing thrust, acted like a pump in the test section, aiding the impeller in moving water through the tunnel and increasing the overall flow rate in the tunnel. The higher flow speeds for a given station for the total wake are reflected in the higher average DP readings shown above.

The average DP readings above allowed calculation of calibration factors by which normalized velocities at given points from different rotations could be directly compared for each the nominal and total wakes. Also, normalized velocities from the nominal wake were then compared with those of the total wake through use of an additional calibration factor.

### A.1.1 Nominal Wake

Arbitrarily, the zero degree rotation(deck upright, model port side to laser), was chosen as the "undisturbed" rotation by which the other rotations would be calibrated. To convert a normalized velocity from the 90 degree rotation, for example, that velocity was multiplied by the ratio of the average DP from 90 degrees over the average DP from 0 degrees. For the numbers listed above, a normalized velocity from the 90 degree rotation for the nominal wake would be multiplied by

$$\frac{18.33(average\ DP\ for\ 90\ degree\ rotation)}{18.98(average\ DP\ for\ 0\ degree\ rotation)} = 0.97.$$

The calibration factors for the 180 and 270 degree rotations were found likewise by replacing the average DP for 90 degrees by the average DP for 180 degrees or the average DP for 270 degrees, respectively. The calibration factor for the 0 degree rotation is 1.00.

### A.1.2 Total Wake

The process for the total wake was identical to that above for the nominal wake, only using the average DP readings for each rotation from the unsteady total wake data collection sessions. These readings are shown above. Like the nominal wake calibration, a normalized velocity from the 270 degree rotation, for example, was

multiplied by

$$\frac{20.32(average\ DP\ for\ 270\ degree\ rotation)}{19.48(average\ DP\ for\ 0\ degree\ rotation)} = 1.04.$$

The process for the other rotations is as with the nominal wake and again the calibration factor for the 0 degree rotation is 1.00.

### A.1.3 Conglomeration of Data from the Four Rotations

The result of the calibrations was four data files which could be combined/compared with each other for each station for both the nominal and total wake studies. The program listed in Appendix B was used to take the four two-dimensional total wake velocity data files(one for each rotation) for station #3 and combine them into one file which contains three-dimensional velocity data for each test point relative to the model. With slight changes, the program was also used to combine the nominal files from each rotation into one three-dimensional file. As stated in the main text, axial velocities for a given point relative to the model obtained from different rotations were redundant and could be combined/averaged. Vertical velocities relative to the tunnel(which is what the laser measures) resolve to either positive or negative vertical or horizontal velocities in a coordinate system relative to the model. Good examples of this resolution are:

- Vertical velocities relative to the tunnel, taken with the model upside down(180 degree rotation), are actually negative vertical velocities in model coordinates. (See the end of Section 2.3.2 for the definition of vertical and horizontal)

- Vertical velocities relative to the tunnel, taken when the model's deck is toward the laser (90 degree rotation), are actually positive horizontal velocities in model coordinates.

The program used addition and subtraction to combine the velocities at each station from each of the four rotations(for both the nominal and the total wakes) and gave single three-dimensional velocity files. Note that this program could be changed

easily to allow for trigonometric manipulation of the vertical and horizontal velocities at each point to produce radial and tangential velocities if necessary.

### A.1.4 Comparison of Nominal Wake Data with Total Wake Data

The problem remaining was the higher average DP readings for the total wake(due to the pumping of the propeller) which prevented direct comparison of the nominal and total wake files. After the calibration and conglomeration of the data, both the nominal and total wake files contained normalized velocities which, in effect, had been normalized by their respective 0 degree average DP reading. Thus, a final calibration was determined to convert the total wake normalized velocities to allow direct comparison with the nominal wake normalized velocities. This was accomplished with a calibration factor based upon the average DP reading for the total wake 0 degree rotation and the average DP reading for the nominal wake 0 degree rotation. The total wake normalized three-dimensional velocities for station #3 were multiplied by

$$\frac{19.48(0\ \textit{degree total wake average DP reading})}{18.98(0\ \textit{degree nominal wake average DP reading})} = 1.03.$$

The result was three-dimensional normalized velocity data for station #3 from which direct comparisons between the nominal and total wakes could be made. This same procedure was used for other stations as well, using the respective average DP readings from those stations.

# Appendix B

# Data Manipulation Codes

## B.1 Conglomeration of the Four Rotations

```
c       program UNCONGL.F
c
c       Todd Taylor
c       11/11/92,3/30/93

c.....This program will take unsteady data
c.....for each of the four rotations (of a given
c.....station) and combine the velocities by resolving directions
c.....of one cut with respect to another and averaging where there
c.....are duplicate velocities for the same point.                    10


      real vx0(10,19),vz0(10,19),vx90(10,19),vz90(10,19)
      real vx180(10,19),vz180(10,19),vx270(10,19),vz270(10,19)
      real va(10,36),vv(10,36),vh(10,36),rad,ang,x,y,a,b
      character*80 infile1,infile2,infile3,infile4,ofile
      integer iradius,iangle


c                                                                     20
c.....vx0(i,j) is the normalized axial velocity from the
```

```
c       0 degree rotation
c.....vz0(i,j) is the normalized vertical velocity from the
c       0 degree rotation
c.....(and so on for 90,180 270)
c.....va(i,j) is the total normalized axial velocity
c.....vv(i,j) is the total normalized vertical velocity
c.....vh(i,j) is the total normalized horizontal velocity
c.....i, the first index, is the (radius in mm/108)
c.....j, the second index, is (angle in degrees/10)+1                    30
c.....x,y are cartesian coordinates for plotting the data

      write(*,*) 'Name of 0 degree input file:'
      read(*,'(a)') infile1
      write(*,*) 'Name of 90 degree input file:'
      read(*,'(a)') infile2
      write(*,*) 'Name of 180 degree input file:'
      read(*,'(a)') infile3
      write(*,*) 'Name of 270 degree input file:'
      read(*,'(a)') infile4                                              40
      write(*,*) 'Name of output file?'
      read(*,'(a)') ofile

      open(unit=11,file=infile1,status='unknown')
      open(unit=12,file=infile2,status='unknown')
      open(unit=13,file=infile3,status='unknown')
      open(unit=14,file=infile4,status='unknown')
      open(unit=15,file=ofile,status='unknown')

c.....normalized data files from which to read have been opened          50


c.....READ IN 0 DEGREE FILE

      do 100 iradius=10,1,-1

      do 90 iangle=1,19
```

```
      read(11,*,err=101,end=101)a,b,vx0(iradius,iangle),
&     vz0(iradius,iangle)                                              60

 90   continue
100   continue
101   continue

c.....READ IN 270 DEGREE FILE

      do 200 iradius=10,1,-1

      do 190 iangle=1,19                                               70

      read(14,*,err=201,end=201)a,b,vx270(iradius,iangle),
&     vz270(iradius,iangle)

190   continue
200   continue
201   continue

c.....READ IN 180 DEGREE FILE

                                                                       80
      do 300 iradius=10,1,-1

      do 290 iangle=1,19

      read(13,*,err=301,end=301)a,b,vx180(iradius,iangle),
&     vz180(iradius,iangle)

290   continue
300   continue
301   continue                                                         90

c.....READ IN 90 DEGREE FILE
```

```
      do 400 iradius=10,1,-1

      do 390 iangle=1,19

      read(12,*,err=401,end=401)a,b,vx90(iradius,iangle),
&      vz90(iradius,iangle)
                                                                    100
390   continue
400   continue
401   continue


c.....
c.....THE 4 FILES ARE NOW IN MEMORY
c.....
c.....major axes (deck, keel, port, starboard) done separately
c.....                                                              110


c.....COMBINE VELOCITIES FOR THE FOUR QUADRANTS

c.....first quadrant (port deck)
c.....0 and 90 degree axes in common

      do 510 iradius=10,1,-1
                                                                    120
      do 509 iangle=2,9

      ia90=iangle+9

      va(iradius,iangle)=(vx0(iradius,iangle)+vx90(iradius,ia90))/2.
      vv(iradius,iangle)=vz0(iradius,iangle)
      vh(iradius,iangle)=vz90(iradius,ia90)

509   continue
```

```
510   continue                                                          130

c.....second quadrant (port keel)
c.....0 and 270 degree axes in common

      do 520 iradius=10,1,-1

      do 519 iangle=11,18

      ia270=iangle-9
                                                                        140
      va(iradius,iangle)=(vx0(iradius,iangle)+vx270(iradius,ia270))/2.
      vv(iradius,iangle)=vz0(iradius,iangle)
      vh(iradius,iangle)=(-1.)*(vz270(iradius,ia270))

519   continue
520   continue

c.....third quadrant (starboard keel)
c.....270 and 180 degree axes in common
                                                                        150
      do 530 iradius=10,1,-1

      do 529 iangle=20,27

      ia270=iangle-9
      ia180=iangle-18

      va(iradius,iangle)=(vx270(iradius,ia270)+vx180(iradius,ia180))/2.
      vv(iradius,iangle)=(-1.)*(vz180(iradius,ia180))
      vh(iradius,iangle)=(-1.)*(vz270(iradius,ia270))                   160

529   continue
530   continue

c.....fourth quadrant (starboard deck)
```

```
c.....90 and 180 degree axes in common

      do 540 iradius=10,1,-1

      do 539 iangle=29,36                                              170

      ia180=iangle-18
      ia90=iangle-27

      va(iradius,iangle)=(vx90(iradius,ia90)+vx180(iradius,ia180))/2.
      vv(iradius,iangle)=(-1.)*(vz180(iradius,ia180))
      vh(iradius,iangle)=vz90(iradius,ia90)

539   continue
540   continue                                                         180

c.....

c.....CALCULATION OF VELOCITIES ON THE AXES
C.....




c.....deck axis
c.....0,90,180 degree axes in common                                   190

      do 550 iradius=10,1,-1

      iangle=1
      ia0=iangle
      ia90=10
      ia180=19

      va(iradius,iangle)=(vx0(iradius,ia0)+vx90(iradius,ia90)
&      +vx180(iradius,ia180))/3.                                       200
      vv(iradius,iangle)=(vz0(iradius,ia0)-vz180(iradius,ia180))/2.
```

```
      vh(iradius,iangle)=vz90(iradius,ia90)

550   continue

c.....port axis
c.....90,0,270 degree axes in common

      do 560 iradius=10,1,-1                                          210

      iangle=10
      ia90=19
      ia270=1

      va(iradius,iangle)=(vx0(iradius,iangle)+vx90(iradius,ia90)
&      +vx270(iradius,ia270))/3.
      vv(iradius,iangle)=vz0(iradius,iangle)
      vh(iradius,iangle)=(vz90(iradius,ia90)-vz270(iradius,ia270))/2.

560   continue                                                        220


c.....keel axis
c.....0,270,180 degree axes in common

      do 570 iradius=10,1,-1

      iangle=19
      ia0=iangle
      ia270=10                                                        230
      ia180=1

      va(iradius,iangle)=(vx0(iradius,ia0)+vx270(iradius,ia270)
&      +vx180(iradius,ia180))/3.
      vv(iradius,iangle)=(vz0(iradius,ia0)-vz180(iradius,ia180))/2.
      vh(iradius,iangle)=-vz270(iradius,ia270)
```

```
570   continue

                                                                      240
c.............starboard axis
c.............90,180,270 degree axes in common

      do 580 iradius=10,1,-1

      iangle=28
      ia90=1
      ia180=10
      ia270=19
                                                                      250
      va(iradius,iangle)=(vx90(iradius,ia90)+vx180(iradius,ia180)
&      +vx270(iradius,ia270))/3.
      vv(iradius,iangle)=-vz180(iradius,ia180)
      vh(iradius,iangle)=(-vz270(iradius,ia270)+vz90(iradius,ia90))/2.

580   continue

c.....
c.............all point velocities have been calculated/averaged
c.....                                                                260

c.....
c.............OUTPUT   OUTPUT   OUTPUT.....
c.............write out whole file by x,y,va,vv,vh
c.....

      do 700 iradius=10,1,-1

      do 690 iangle=1,36
                                                                      270
      rad=((iradius+2.)/10.)*108.17
      ang=((iangle-1.)*10.)*(3.1415927/180.)
```

```
      x=-rad*(sin(ang))
      y=rad*cos(ang)

c.....remove numerical error
      if (abs(x).lt.1) then
      x=0.000
      else if (abs(y).lt.1) then                                        280
      y=0.000
      end if
c.....


      write(15,800)x,y,va(iradius,iangle),vv(iradius,iangle),
&      vh(iradius,iangle)

                                                                        290
690   continue

c.....add in deck axis again for tecplot closure:
c.....these three lines are specific to form needed for MIT
c.....plotting routines.....

      x=0.
      y=((iradius+2.)/10.)*108.17
       write(15,800)x,y,va(iradius,1),vv(iradius,1),vh(iradius,1)
                                                                        300
C.....
C.....

700   continue
710   continue

800   format(x,f8.3,x,f8.3,x,f10.6,x,f10.6,x,f10.6)
```

```
      stop                                                          310
      end
```

```
                                                                    320
```

## B.2 Preparation of Wake Files for WAKEPROC

```
c.....Program PROCPREP
c
c.....Todd Taylor
c.....
c..This program will take a nominal wake file (station #3)
c..and convert it into the form needed by the 'wakeproc' code.


c....Variables
c.....                                                              10

      real x(13,73),y(13,73),va(13,73),vv(13,73),vh(13,73)
      real vtheta(13,72),vrad(13,72),irads
      integer i,j
      character*80 junk

c.....
c....x=x position
c....y=y position
c....va=axial(downstream) velocity                                  20
c....vv=vertical(upward) velocity
c....vh=horizontal(toward back of tunnel) velocity
c....vtheta=circumferential velocity
c....vrad=radial velocity
c....irads=angle of postion in radians
c.....
c.....

      open(unit=11,file='whole3.dat',status='unknown')
      open(unit=12,file='proc3.dat',status='unknown')               30

c....discard headers

      read(11,'(a)') junk
```

```
      read(11,'(a)') junk
      read(11,'(a)') junk

c....read in data
c....data is grouped by radius and then by angles of 5 degrees
      do 100 i=13,1,-1                                                  40

      do 200 j=1,72

        read(11,*)x(i,j),y(i,j),va(i,j),vv(i,j),vh(i,j)


c.....angle in rads

        irads=((j-1)/72)*(2*3.141592)
                                                                        50

c.....
c.....Process data by 'quadrants' relative to model
c.....For example, upper left is the port deck quadrant
c.....

c.....upper left quadrant

        if (j .lt. 20) then
          vtheta(i,j)=-vh(i,j)*cos(irads)-vv(i,j)*sin(irads)            60
          vrad(i,j)=vv(i,j)*cos(irads)-vh(i,j)*sin(irads)
        end if

c.....lower left quadrant

        if ((j .lt. 38).and.(j .gt. 19)) then
           irads=irads-(3.141592/2)
           vtheta(i,j)=-vv(i,j)*cos(irads)+vh(i,j)*sin(irads)
           vrad(i,j)=-vh(i,j)*cos(irads)-vv(i,j)*sin(irads)
        end if                                                          70
```

```
c.....lower right quadrant

      if((j .lt. 56).and.(j .gt. 37)) then
         irads=irads-3.141592
         vtheta(i,j)=vv(i,j)*sin(irads)+vh(i,j)*cos(irads)
         vrad(i,j)=-vv(i,j)*cos(irads)+vh(i,j)*sin(irads)
      end if

c.....upper right quadrant                                          80

      if(j .gt. 55) then
         irads=irads-((1.5)*3.141592)
         vtheta(i,j)=vv(i,j)*cos(irads)-vh(i,j)*sin(irads)
         vrad(i,j)=vv(i,j)*sin(irads)+vh(i,j)*cos(irads)
      end if

 200  continue

c.....Get rid of foldover(closure) line from tecplot applications.  90
c.....(Tecplot needs the first data point(0 degrees) for a given
c.....radius repeated as the last data point(360 degrees) for
c.....that radius so that the software understands which points
c.....actually fall near each other in model coordinates.)

      read(11,*)a,b,c,d,e

 100  continue

c.....OUTPUT.....                                                   100
c.....
c.....Write out the
c.....header to file for WKPROC
      write(12,'(a)')'Hyundai Station\#3,3 component for WKPROC, 13radii,
& 72angles'
      write(12,'(a)')'1 1 1 1'
```

```
c       write(12,'(a)')'1'
c       write(12,'(a)')'1'
c       write(12,'(a)')'1'
                                                                      110
c.....Write out the # of radii, # of angles,  and their lists
c.....to the file

      call POINTS

c.....write out axial velocities
      do 300 i=1,13
      do 400 j=1,72,6

        write(12,600)va(i,j),va(i,j+1),va(i,j+2),va(i,j+3),va(i,j+4)   120
&         ,va(i,j+5)

 400      continue
         write(12,*)' '
 300      continue


c.....write out radial velocities

         call POINTS                                                  130

        do 402 i=1,13
        do 403 j=1,72,6

        write(12,600)vrad(i,j),vrad(i,j+1),vrad(i,j+2),vrad(i,j+3)
&         ,vrad(i,j+4),vrad(i,j+5)

 403      continue
         write(12,*)' '
 402      continue                                                    140

c.....write out tangential velocities
```

```
      call POINTS

      do 410 i=1,13
      do 411 j=1,72,6

        write(12,600)vtheta(i,j),vtheta(i,j+1),vtheta(i,j+2)
&       ,vtheta(i,j+3),vtheta(i,j+4),vtheta(i,j+5)                    150

411     continue
        write(12,*)' '
410     continue

600   format(f8.6,2x,f8.6,2x,f8.6,2x,f8.6,2x,f8.6,2x,f8.6)

      stop
      end
                                                                      160

c.....Subroutine to print angles and radii

      subroutine POINTS

c.....There are 13 radii, 72 angles(0-360)

      write(12,'(a)')'13 72'

c**********radii written inner to outer******************            170
      write(12,'(a)')'0.2496 0.3328 0.4160 0.4992 0.5824 0.6656'
      write(12,'(a)')'0.7488 0.8320 0.9152 0.9984 1.0816 1.1648'
      write(12,'(a)')'1.2480'
c*********************************************************
      write(12,*)' '

c*************Angles in degrees clockwise looking downstream********
      write(12,'(a)')'0.0 5.0 10.0 15.0 20.0 25.0 30.0 35.0 40.0 45.0'
```

```
      write(12,'(a)')'50.0 55.0 60.0 65.0 70.0 75.0 80.0 85.0 90.0'
      write(12,'(a)')'95.0 100.0 105.0 110.0 115.0 120.0 125.0 130.0'                180
      write(12,'(a)')'135.0 140.0 145.0 150.0 155.0 160.0 165.0 170.0'
      write(12,'(a)')'175.0 180.0 185.0 190.0 195.0 200.0 205.0 210.0'
      write(12,'(a)')'215.0 220.0 225.0 230.0 235.0 240.0 245.0 250.0'
      write(12,'(a)')'255.0 260.0 265.0 270.0 275.0 280.0 285.0 290.0'
      write(12,'(a)')'295.0 300.0 305.0 310.0 315.0 320.0 325.0 330.0'
      write(12,'(a)')'335.0 340.0 345.0 350.0 355.0'
c**********************************************************************
      write(12,*)' '

      return                                                                         190
      end
```

## B.3 Conversion of Propeller Offsets

```
      program rakecalc

c.....This program takes model propeller offsets which are listed
c.....with a convention showing zero rake and converts them to the
c.... MIT convention for rake.

c.....Todd Taylor 2/3/93

c.....VARIABLES.....

      real diam, radius, pitch,skewdeg,rakemc
      real rakediam,skewrad,tanpitch
      real radratio

c..rakemc=rake at midcord of the blade at radius under consideration
c..diam=diameter of prop(mm)
c..radius=radius of prop(mm)
c..pitch=(mm) of pitch at radius under consideration
c..skewdeg=degrees of skew at radius under consideration
c..rakediam=rake to diameter ratio
c..skewrad=radians of skew at radius under consideration

      diam=8200.0
      radius=4100.0

c.....for 10 radii.....

      do 20 i=1,10

      write(*,*)'Input current radius(mm), skew angle(deg), pitch(mm)'
      Read(*,*)radius,skewdeg,pitch

      tanpitch=((pitch/diam)/3.1415927)
      skewrad=(skewdeg/360)*(2*3.1415927)
```

```
      rakemc=radius*skewrad*tanpitch
      rakediam=rakemc/diam
      radratio=(radius/(diam/2))
      write(*,*)'radius= ',radius
      write(*,*)'r/R= ',radratio                                    40
      write(*,*)'Rake-MC= ',rakemc
      write(*,*)'rake/diam= ',rakediam

 20   continue

c.....GL-MC = (r*skewrad)/cos(pitchangle))

                                                                    50

      stop
      end
```

# Appendix C

# Model Propeller Dimensions

The full scale propeller has a diameter of 8200.0mm, five blades, and an expanded area ratio of 0.8537. It has a pitch at 0.7R of 8851.9mm, a mean pitch of 8429.1mm and a hub ratio(DH/D) of 0.220. The model propeller, with a diameter of 216.3mm, is a 1/37.903 scale of the full scale propeller.

Shown in Table C.1 are the model propeller dimensions, in millimeters unless otherwise noted.

| r/R | Pitch | Rake | Skew(degrees) | Chord | Max Camber | Max Thickness |
|---|---|---|---|---|---|---|
| 0.220 | 180.7 | 0.00 | 0.00 | 59.6 | 2.5 | 9.1 |
| 0.250 | 190.5 | -8.08 | -1.61 | 62.1 | 2.5 | 8.7 |
| 0.300 | 203.0 | -23.01 | -3.59 | 66.2 | 2.6 | 8.0 |
| 0.400 | 219.8 | -47.19 | -5.10 | 73.5 | 2.4 | 6.8 |
| 0.500 | 228.6 | -45.14 | -3.75 | 79.5 | 1.9 | 5.5 |
| 0.600 | 233.1 | -0.43 | -0.03 | 83.7 | 1.5 | 4.3 |
| 0.700 | 233.5 | 96.04 | 5.58 | 85.3 | 1.3 | 3.3 |
| 0.800 | 229.1 | 243.03 | 12.59 | 82.9 | 1.1 | 2.6 |
| 0.900 | 218.9 | 425.75 | 20.53 | 72.3 | 0.8 | 1.5 |
| 0.950 | 210.1 | 518.82 | 24.69 | 59.3 | 0.4 | 1.0 |
| 1.000 | 196.3 | 597.26 | 28.90 | 0.0 | 0.0 | 0.6 |

Table C.1: Model Propeller Dimensions

# Bibliography

[1] T.E. Brockett. Shear flow effects on propeller operation: Effective velocity, loads and vortex sheet geometry. Technical Report 294, Department of Naval Architecture and Marine Engineering, University of Michigan, Ann Arbor, 1985.

[2] Elizabeth Ann Horwich. Unsteady response of a two-dimensional hydrofoil subject to high reduced frequency gust loading. Master's thesis, Massachusetts Institute of Technology, June 1993.

[3] Stanley L. Kaufman. Fiberoptics in laser doppler velocimetry. *Lasers and Applications*, July 1986.

[4] J.E. Kerwin and C.-S. Lee. Prediction of steady and unsteady marine propeller performance by numerical lifting-surface theory. *Society of Naval Architects and Marine Engineers Transactions*, 86:218–253, 1978.

[5] Justin E. Kerwin. Marine propellers. *Annual Review of Fluid Mechanics*, 1986.

[6] J.N. Newman. *Marine Hydrodynamics.* MIT Press, Cambridge, Massachusetts, 1977.

[7] Nancy C. Groves Thomas T. Huang. Effective wake: Theory and experiment. Technical Report DTNSRDC-81/033, David W. Taylor Naval Ship Research and Development Center, Bethesda, MD, 1981.